



27

28 **Abstract** – The stratified nature of tropical forest structure had been noted by early explorers,  
29 but until recent use of satellite-based LiDAR (GEDI, or Global Ecosystems Dynamics  
30 Investigation LiDAR), there has been no way to quantify stratification across all tropical forests.  
31 Understanding stratification is important because by some estimates, a majority of the world’s  
32 species inhabit tropical forest canopies. Stratification can modify vertical microenvironment, and  
33 thus can affect a species’ susceptibility to global warming. A better understanding of structure  
34 could also improve predictions of biomass across the tropics. Here we find that, based on  
35 analyzing each GEDI 25m diameter footprint in tropical forests (after screening for human  
36 impact), most footprints (60-90%) do not have multiple layers of vegetation. This result is  
37 highly scale dependent, but with a 25m footprint, the most common forest structure has a  
38 minimum plant area index (PAI) at ~40m followed by an increase in PAI until ~15m followed by  
39 a decline in PAI to the ground layer (described hereafter as a one peak footprint). However,  
40 there are large geographic patterns to forest structure within the Amazon basin (ranging between  
41 60-90% one peak) and between the Amazon ( $79\pm 9\text{sd}$ ) and SE Asia or Africa ( $72\pm 14$  v  $73\pm 11$ ).  
42 The number of canopy layers is significantly correlated with tree height ( $r^2=0.12$ ), forest biomass  
43 ( $r^2=0.14$ ), maximum temperature ( $T_{\text{max}}$ ) ( $r^2=0.05$ ), vapor pressure deficit (VPD) ( $r^2=0.03$ ) and  
44 soil fertility proxies (e.g. total cation exchange capacity - $r^2=0.01$ ). Certain boundaries, like the  
45 Pebas Formation and Ecoregions, clearly delineate continental scale structural changes. More  
46 broadly, deviation from more ideal conditions (e.g. lower fertility or higher temperatures) leads  
47 to shorter, less stratified forests with lower biomass.

48

49

50

## 51 **Introduction**

52 Early Western visitors describe tropical forests as *horror vacui* (nature abhorring a  
53 vacuum) since vegetation was “anxious to fill every available space with stems and leaves”,  
54 which was a change from more open temperate forests (Richards, 1952). However, a closer  
55 examination of tropical forests revealed structure or stratification with “a discernible, though  
56 complicated, arrangement in space” (Richards, 1952). Halle et al 1980 built on this with their  
57 influential work identifying twenty-three unique tree architecture types and delving into the  
58 drivers of forest architecture (Halle, Oldeman and Tomlinson, 1980). They recognized that  
59 because tropical forests had fewer hydraulic or cold temperature constraints, the tropics was a  
60 good place to study the potential for trees to fill vertical space. They developed theories using  
61 detailed 20 by 30m vertical profiles of old growth canopies where “trees of the present” occupy  
62 space in the upper canopy as well as in a second layer of increased light at 15-20m where  
63 sunflecks converge. This old growth forest architecture would result in a stratified or layered  
64 forest (artistically rendered in Figure 1) unlike younger pioneer forests with a single upper  
65 canopy strata. We define a stratified or multilayer forest as having two or more peaks (e.g.  
66 overstory and midstory in Fig 1) with a lower amount of vegetation between them. Others have  
67 quantified stratification in different ways and found both temperate and tropical forests  
68 commonly have 2-3 tree layers (Baker and Wilson, 2000). However, tropical forest stratification  
69 has not been addressed previously at high spatial resolutions at the global scale.

70 More recently, the Global Ecosystems Dynamic Investigation (GEDI) on the  
71 International Space Station (ISS)-based LiDAR instrument (Dubayah *et al.*, 2020), allows us for  
72 the first time to peer into the structure of tropical forests in unprecedented resolution at a global  
73 scale. Prior to GEDI, there were other satellite lidar instruments (e.g. GLAS on ICESAT-1) used  
74 for measuring vegetation structure at large scale (Tang *et al.*, 2016; Tang and Dubayah, 2017),  
75 but these were lower resolution, much more sparse, and focused on polar regions. At a more  
76 regional scale, aircraft and terrestrial lidar have shown detailed individual tropical forest tree  
77 architectures. For instance, aircraft lidar in tropical Peru found that tree architecture or shape  
78 (height of peak canopy volume (P) divided by canopy height) was highly correlated with canopy  
79 height (Asner *et al.*, 2014) and in Panama others successfully predicted the tree size distributions  
80 with airborne lidar (Taubert *et al.*, 2021). At a global scale, Ehbrecht et al 2021 scaled up  
81 terrestrial laser scanning to show that forest structural complexity is a function of annual  
82 precipitation and precipitation seasonality (Ehbrecht *et al.*, 2021). Both simulation and  
83 sensitivity analysis suggest that high-quality GEDI data is able to provide measurements of  
84 similar accuracy in the tropics when compared to aircraft and terrestrial lidar (Marselis *et al.*,  
85 2018, 2020). We can now use these different lidar tools (from individual tree to global) to  
86 understand how forest stratification changes across the tropics globally.

87 Forest stratification may be due to genetic constraints evolved over time (floristics) or  
88 trees not achieving their genetic heights (environmental or soil constraints). The debate about  
89 what sets the upper limits of tree height largely involves either hydraulic limitation (Koch et al  
90 2004), mechanical limitation, or environmental factors such as wind speed (Jackson *et al.*, 2021).

91 Forest height and structure are also driven by genetics, and evolutionary forces such as the need  
92 to overtop competitors or disperse seeds encourages height and complex structure while risks  
93 such as hydraulic failure and vulnerability to wind discourage it. Environment alone could also  
94 directly impact tree height and structure, with hydraulic limitations, carbon deficiencies, or wind  
95 regimes causing trees to not being able to achieve their genetic height. There is a literature  
96 describing how the environment (soils or climate) impacts the species composition in tropical  
97 forests. For instance, Amazonian species composition may follow a south-west/north-east soil  
98 fertility gradient and a north-west/south-east precipitation gradient (ter Steege *et al.*, 2006). Soil  
99 cation concentrations are the primary driver of floristic variation for Amazonian trees (Tuomisto  
100 *et al.*, 2019) with climate being of secondary importance. However, in central African forests,  
101 climate is considered to be the driving factor of floristic patterns (Réjou-Méchain *et al.*, 2021).

102 Structure matters because it can give us new insights into forest biomass, which is the  
103 primary goal of GEDI. Currently the L4A product for tropical forests uses relative height (RH)  
104 RH98 and RH50 to predict a median AGBD of 300 Mg Ha<sup>-1</sup> for tropical forests (0.66 r<sup>2</sup> and  
105 RMSE of 10.4) (Duncanson *et al.*, 2022). Ecological theory suggests that a stratified forest with  
106 more large emergent trees is indicative of an older forest (Halle, Oldeman and Tomlinson, 1980),  
107 which generally has higher biomass and carbon content. Therefore, incorporating canopy layers  
108 may improve prediction of tropical forest biomass.

109 Finally, understanding tropical forest structure matters, because prior to GEDI, detailed  
110 pan-tropical structural data did not exist and is therefore understudied, and yet it is where the  
111 bulk of the world's species exist (Stork, 2018) including over 75 % of all vertebrates and 60 % of  
112 neotropical mammal species (Kays and Allison, 2001). Structure is indicative of use: for  
113 example, tall canopies were a strong predictor of habitat use by Baldfaced saki monkeys  
114 (*Pithecia irrorata*) in the Peruvian Amazon (Palminteri and Peres, 2012) and structure data are  
115 increasingly being used in species distribution models (Burns *et al.*, 2020). Stratification has  
116 been hypothesized to increase rates of pollination and dispersal, optimize light use, increase  
117 inter-canopy CO<sub>2</sub> concentrations, reduce leaf, fruit and flower predation, and increase forest  
118 structural integrity (Smith, 1973). Overall, structure also creates the habitat for all other forest  
119 dwelling species (Terborgh, 1992). For instance, figure one shows animals both impacting and  
120 being impacted by forest structure.

121 The structure of forests is also a principal factor in determining not just the mean  
122 environment experienced by forest-dwelling organisms, but also the diversity, extent, and  
123 variability of microenvironments. The extent and diversity of microenvironments directly affects  
124 the niches available to organisms, and hence the diversity of forest-dwelling organisms. For  
125 instance, Oliveira and Scheffers (2019) proposed an 'arboreality hypothesis' where species have  
126 increased ranges because they can take advantage of changing microclimates in different canopy  
127 layers as temperatures shift due to elevation and latitude. They further suggested that future  
128 warming may push arboreal species towards the cooler ground layer (Oliveira and Scheffers,  
129 2019). Another study suggested that climate change may cause arboreal species in hot sparse  
130 canopies towards greater ground use (Eppley *et al.*, 2022). Detailed models now exist to predict  
131 canopy microclimate with forest structure as a possible input (Maclean and Klinges, 2021).

132 Therefore, forest structure and related microhabitats becomes even more critical as climate  
133 change progresses.

134 Here we use GEDI to understand tropical forest structure and address the following  
135 hypotheses:

136 **H1** – Most tropical forests (when measured at spatial resolutions of ~25m diameter) exhibit  
137 structure or multi-layered canopies.

138 **H2** – The spatial distribution of canopy structure is controlled by soils (e.g. total cation exchange  
139 capacity) and/or environment (e.g. maximum temperature).

140

141 **Methods**

142 **GEDI data** – We used the vertical forest structure (L2A and L2B, Version 2) and biomass (L4A  
143 – see below) products from the GEDI instrument (Dubayah *et al.*, 2020) based on the ISS  
144 between 2019.04.18 and 2021.02.17 for tropical forest regions (Amazonia, Central Africa, and  
145 SE Asia). We principally used the Plant Area Volume Density (PAVD) profile, defined as the  
146 Plant Area Index (PAI – which incorporates both leaf and wood) separated into 5-meter vertical  
147 bins (which can reduce vertical uncertainty). We applied a number of data filters to ensure  
148 quality such as: degrade flag = 0 (e.g. not in degraded altitude), L2A and L2B quality flags = 1  
149 (simplified metric to only use highest quality data based on energy, sensitivity, amplitude, and  
150 real-time surface tracking quality), sensitivity  $\geq 0.95$ , power beams during night and day and  
151 coverage beams during night only (nights are generally better to remove the negative impact of  
152 background solar illumination). To ensure accuracy, we compared GEDI height to TanDEM-X  
153 (Krieger *et al.*, 2007)(a satellite that employs SAR (synthetic aperture radar) to determine an  
154 object’s height above ground) and only used areas where canopy height  $< 100$  m, and elevation  
155 difference from GEDI is between  $\pm 100$  m. To ensure that the footprints were in tropical forest  
156 regions, we applied four additional filters:

- 157 1. Treecover %  $>90\%$  in the year 2010, defined as canopy closure for all vegetation taller  
158 than 5m (Hansen *et al.*, 2013).
- 159 2. Forests with heights  $>10$ m (but vary this number in a sensitivity study 15, 20, and 25m -  
160 Fig S1) using the relative height metric 98% which was calculated as the height relative  
161 to ground elevation under which 98% percentage of waveform energy has been returned.
- 162 3. The GEDI footprint was classified as Plant Functional Type (PFT) Broadleaf Evergreen  
163 Tropical based on MODIS MCD12Q1v006 Product from 2021 (Friedl *et al.* 2019). Values  
164 follow the Land Cover Type 5 Classification scheme.
- 165 4. We compared an index of forest integrity as determined by degree of anthropogenic  
166 modification <https://www.forestintegrity.com/> (Grantham *et al.*, 2020) to maps of the %  
167 one peak (see below – Fig S2).

168 If the GEDI footprint passed these filters, we analyzed each PAVD profile in a 0.1 by 0.1  
169 degrees size gridcell. Using the Matlab (Mathworks) function “islocalmax”, we identified local  
170 maxima (change in first derivative) in each PAVD profile. We first classified the footprint by  
171 the number of local maxima (hereafter: peaks) (1-3). If it had two peaks, we then classified the  
172 profile whether the first (lower to the ground) or second peak has more PAVD. We then use the  
173 following equation to determine if the peaks are even or if one is much lower than the other:

174 Equation 1 –  $PAVD\_diff = \text{abs}((PAVD \text{ Peak } 1 - PAVD \text{ Peak } 2) / PAVD \text{ Peak } 1) * 100;$   
175

176 We classified each profile separately if PAVD\_diff is  $>50$  or  $<50$ . We classified vertical space  
177 between peaks ( $>10$  m between peaks or less). For instance, for a profile, if two peaks are found,  
178 if the first peak is higher with less than 50% difference between the peaks, it is classified as red  
179 (2p\_eq\_high) (Figs 2-3), if more than 50% difference it is classified as magenta (2p\_eq\_low). If  
180 the second peak is higher with less than 50% difference, it is classified as green (2p\_uneq\_high),  
181 if more than 50% difference yellow (2p\_uneq\_low). If the distance between the peaks is less

182 than 15m it is black (2p\_even). To calculate the percentage of one peak PAVD profiles, we sum  
183 the number of one peak profiles divided by all profiles measured in a 0.1 by 0.1 degree pixel.

184 In addition to classifying these vertical profiles, for each 0.1 by 0.1 degree subregion, for all tree  
185 heights (RH98) that pass our filters, we create a histogram, and the peak of the histogram is  
186 classified as median rh98 tree height. For each 0.1 by 0.1 degree subregion, we estimate the total  
187 plant area index (PAI) as a proxy for commonly used metrics like leaf area index (LAI). We  
188 downloaded the GEDI L4B above ground biomass density (AGBD) product from DAAC  
189 ([https://daac.ornl.gov/cgi-bin/dsviewer.pl?ds\\_id=2017](https://daac.ornl.gov/cgi-bin/dsviewer.pl?ds_id=2017)) and averaged it for each 0.1 by 0.1  
190 degree pixel.

191 **Plot data** –To ground validate our GEDI stratification results, we estimated crown area using  
192 measured individual tree height and DBH for plots in six diverse regions of the Amazon basin  
193 (Caxiuana 4 ha – 2250 trees >10cm DBH, Tambopata 2ha – 1367 trees>10cm DBH, Iquitos 2ha  
194 1165 trees>10cm DBH, Tapajos – 18ha- 1036 trees>25cm DBH, Bolivia 2ha 974 trees>10cm  
195 DBH, Tanguro 1 ha – 366 trees>10cm DBH)(Doughty *et al.*, 2015). Plot locations are shown as  
196 black dots in Figure 2. For each plot, we used tree height in each 5-meter tree height bin (5-35m)  
197 to estimate crown diameter following Asner et al 2002, shown below as Eq 2 where DBH is the  
198 diameter at breast height (cm) and crown diameter is in meters.

199 Equation 2 - Crown diameter (m) =  $9.3 \cdot \ln(\text{DBH (cm)}) - 22.2$ ;

200

201 We estimate crown area to ground area ratio for all trees in the plots (e.g. Iquitos 2 ha = 1165  
202 trees>10 cm DBH) and on a subset of groups of 50 trees to better approximate the 25 m size of a  
203 GEDI footprint, as this is an approximate average number of trees >10cm DBH per 25m  
204 diameter circle in the tropics. For instance, a typical one hectare tropical forest plot would  
205 contain between 500-1000 trees with DBH>10cm (Malhi *et al.*, 2021) (~20 GEDI footprints if  
206 evenly spaced – which would not happen in practice) and each footprint, therefore, might contain  
207 25-50 trees (with DBH>10cm). We then use the same “peak” procedure (Eq 1 - described above)  
208 to estimate % one peak as a percentage for each region. We estimate crown area to ground area  
209 for each 5-meter bin and vertically area summed. We also show median and maximum tree  
210 height for the plots.

211 For a broader range of plots in the GEM network (listed in Table 1) (Malhi *et al.*, 2021), we  
212 found the PAVD profile for the footprint closest to the plot as well as all footprints within a  
213  $0.03^\circ$  grid around the plot coordinates. Most of these plots had in situ leaf traits measured to  
214 account for 70-80% of the basal area (of trees >10cm DBH) of 1 ha plots. Plant leaf traits have  
215 been related to plot level architecture in the tropics and predicted with leaf spectral data  
216 (Doughty *et al.*, 2017). We therefore hypothesized that optically derived leaf trait predictions  
217 may predict structure at the landscape scale. Based on the above described field campaigns,  
218 (Aguirre-Gutiérrez *et al.*, 2021) used Sentinel-2 to create remotely sensed canopy trait maps for  
219 P=phosphorus %, WD = wood density  $\text{g}\cdot\text{cm}^{-3}$ , and SLA=specific leaf area  $\text{m}^2 \text{g}^{-1}$ . We then  
220 compared the GEDI profile (% one peak) to the trait value predicted by those maps to that  
221 footprint.

222 **Other data layers** – We compared % one peak to several other climate, soils, and ecoregion  
223 maps listed below for the Amazon basin. We currently focus on the drivers of structure and  
224 validating GEDI for the Amazon region in this paper, but follow on papers may do a similar  
225 analysis for Africa and SE Asia. Each dataset had its own resolution, which we standardized to  
226 0.1 by 0.1 degrees.

227 *Ecoregions* - Ecoregions reflect the distributions of a broad range of fauna and flora across the  
228 entire planet and we use them as a proxy for plant biogeography  
229 <https://www.sciencebase.gov/catalog/item/508fece8e4b0a1b43c29ca22> - (Olson *et al.*, 2001).

230 *Soils* – We used data from soilgrids <https://www.soilgrids.org/> (Batjes, Ribeiro and van Oostrum,  
231 2020). We focused on total cation exchange capacity at pH 7 from 0-5cm in units of mmol(c)/kg  
232 as previous studies had suggested this to be an important variable to explain floristic composition  
233 (Figueiredo *et al.*, 2018).

234 *Climate* – We averaged TerraClimate (Abatzoglou *et al.*, 2018)  
235 <https://www.climatologylab.org/terraclimate.html> data between 2000 and 2018 for Climatic  
236 water deficit (CWD) (the difference between monthly reference evapotranspiration calculated  
237 using the Penman Monteith approach and actual evapotranspiration), Vapor Pressure Deficit  
238 (VPD in kPa), Mean Monthly Precipitation (mm/month), potential evapotranspiration (PET) and  
239 maximum and minimum temperature (°C). These data were originally based on CRU Ts4.0 data  
240 and modified by Abatzoglou et al 2018.

241 *Statistical analysis* – For comparison of either single or multiple variables to percent one peak  
242 we used the matlab function “fitlm” to fit linear models and “fitnlm” for the non-linear models.  
243 The P values listed are for the *t*-statistic of the two-sided hypothesis test.

244

245

## 246 **Results**

247 Most individual GEDI footprints in tropical forests do not have multiple layers (as in Fig  
248 1) and instead have a single peak in vegetation density at ~15m, but this ranged geographically  
249 (regionally and between continents) between 60 to 90% (Figs 2-3). Within the Amazon basin  
250 (Figure 1), the broad geographic patterns were a large central region with low stratification,  
251 surrounded by another broad region with greater stratification bordered to the west by the Pebas  
252 formation (Higgins et al 2011), to the east by the Tapajos River, and the South at ~12°S.  
253 Another region of lower stratification occurred towards the southeast in the “arc of  
254 deforestation” and savanna transition zones. River floodplains also tended towards increased  
255 stratification. The Congo basin showed a broadly similar spatial orientation with a central area  
256 with lower stratification surrounded by regions with greater stratification. The floodplains again  
257 were areas with greater stratification. Southeast Asia, composed of mainly islands, showed  
258 greater stratification towards the island center. The island of New Guinea had increasing  
259 stratification moving northward.

260 A low PAI peak (e.g. ~15m) may also indicate forest disturbance due to selective logging  
261 or other human impact. For instance, there was selective logging in parts of Borneo (Riutta *et*  
262 *al.*, 2018) and this impacted structure by increasing the dominance of shorter pioneer one-peak  
263 forests (i.e. Bornean logged plots are 78 % one peak versus 44% for old growth forests).  
264 However, the filters we used (tree height, MODIS PFT, logging product) should remove most  
265 human impact (although there may be older legacy effects we cannot account for). We tested this  
266 by increasing the minimum tree height (between 15, 20 and 25m) and did not see a big impact on  
267 the broader results, although there were minor changes at the 25m threshold (Fig S1). We also  
268 show comparisons of percentage of one peak to a forest disturbance product (Grantham *et al.*,  
269 2020), which showed large regions dominated by one peak forests in areas of minimal human  
270 disturbance (Fig S2).

271 On a subset of the Amazon (5 by 5° black box regions chosen to represent the broader  
272 region in Fig 2 and 3), we averaged the vertical profile for each footprint in each of six structural  
273 categories (see methods) and found “one peak” forests peaked in PAVD at 15m with a fairly  
274 linear decline going upwards until ~40m (Figure 2 blue line). The next most common profile  
275 type (Figure 2 red line -2p\_eq\_high) in the Amazon, in the region of interest, was a “2 peak”  
276 forest (at ~5% of the results), with an initial peak in PAI at 15m and a second lesser peak in PAI  
277 at 30m and a local minimum at 20m. Average forest height of this forest type exceeded the one  
278 peak forests with a maximum height at ~45m versus 40m. This forest type ranged between 1 to  
279 10% of forest pixels and was more abundant in the Southeast and Northwest of the Amazon (Fig  
280 6 – similar figure for Central Africa is Fig S3 and SE Asia Fig S4). The third most common  
281 forest structure (represented by the black line (2p\_even) at 3.2%) had two close peaks at 15 and  
282 25m, with a small nadir at 20m. This forest type had a PAI peak at 25m and was followed by a  
283 steep drop at ~40m. This forest type ranged between 1 and 5% across the Amazon and was  
284 widely dispersed throughout the Basin. The next most common 2-peak structure (magenta  
285 (2p\_eq\_low) in Fig 2) at ~3.2% of forest types with a peak at 15 m followed by a much weaker

286 peak with less than 50% of the PAVD at 30m. This had a similar distribution to the “red  
287 (2p\_eq\_high)” line, but with an additional hotspot in the Southeast that was not present in the  
288 “red (2p\_eq\_high)” (Fig 6). The remaining forest types had greater PAVD in the upper canopy  
289 with peaks at ~30m.

290 To ground truth our results, for six locations (shown as black dots in Fig 2), we used  
291 DBH, tree height, and a canopy diameter model (Asner et al 2002) to estimate that total  
292 vertically summed crown area/ground area averaged  $1.8 \text{ m}^2 \cdot \text{m}^{-2}$  (0.96-2.3 min max). Averaging  
293 all the structure for trees >10cm DBH (>25cm for the Tapajos) in the plots (size ranging between  
294 2 ha to 18 ha) showed a single peak that averaged 20m (between 17.5-22.5m) in crown area/  
295 ground area (thick lines in Figure 4). This 20m height may be taller than the GEDI mean of 15m  
296 due to the absence of smaller 0-10cm DBH trees measured at the plots. We then subsampled 50  
297 trees from each plot (a better approximation for the GEDI footprint size) and more stratification  
298 resulted. For these subsets, we calculated one peak/all data and found a low in Tambopata of  
299 56% one peak to a high of 95% one peak in the Tapajos with the other sites ranging between 73  
300 to 77% one peak, which is a good approximation of percentage one-peak across the Amazon  
301 basin (~79%) (Figure 2). The Tapajos results must be viewed with caution because only large  
302 trees (>25cm DBH) were recorded, which led to a very high percentage one peak. According to  
303 Fig 2, Tambopata and the Tapajos are near regions divided between areas of high and low  
304 structure and most other plots are in areas of less structure (Figure 2).

305 How representative is the structure in plot networks compared to the broader Amazon?  
306 To answer this, we compare GEDI footprints (closest footprint and all footprints averaged within  
307  $0.03^\circ$  radius of the plots) to a well-studied plot network (GEM - (Malhi *et al.*, 2021) in tables 1  
308 and 2) and found the GEDI footprint nearest to the plots showed a gradient from the Western  
309 Amazon (90% one peak), Eastern Amazon (85%), Gabon (80%), to Borneo (50%). Averaging  
310 all nearby footprints showed similar (except for Gabon), but generally lower trends: Western  
311 Amazon (84%), Eastern Amazon (79%), Gabon (54%), and Borneo (61%). In Table one, we  
312 show data for each individual plot along with remotely sensed trait data (Aguirre-Gutiérrez *et al.*,  
313 2021) calibrated from in situ measurements at the plot network, and we found a significant  
314 relationship between structure and SLA ( $r^2=0.12$ ,  $P<0.05$ , %one peak= $-68 \cdot \text{SLA} + 1.4$ ) but not  
315 with wood density and %P. However, this is a global analysis, and the signal is dependent on  
316 low SLA values along an elevation gradient where GEDI is less accurate because of difficulty in  
317 discerning the ground layer. In Borneo, the GEM plot network (Riutta *et al.*, 2018) is along a  
318 logging gradient with a clear change in structure (78 % one peak for logged plots versus 44%  
319 one peak for old growth forests). We found a significant increase in SLA ( $P<0.05$ ) with  
320 disturbance and a close to significant increase in %P with disturbance ( $P=0.06$ ).

321 We compared the average PAVD profiles from the entire Amazon to the average PAVD  
322 profiles for the entire SE Asia and Africa (average continental scale 0.1 by 0.1 degree pixels and  
323 not just the black boxes in figs 2 and 3). On average, the Amazon had greater percent of one  
324 peak forests ( $79 \pm 9 \text{sd}$ ) than either SE Asia or Africa ( $72 \pm 14$  v  $73 \pm 11$ ). Median tree height (rh98)  
325 was lower in the Amazon at 25.6m than in Africa at 28.5m or SE Asia at 28.7m. In the black  
326 box regions shown in Fig 3 for Africa and SE Asia, one peak forests were most abundant (~70%)

327 with a similar peak at 15m (Figure 5). In both the Africa and SE Asia subplots, both red  
328 (2p\_eq\_high) and magenta (2p\_eq\_low) structure types were much more common forest  
329 structures than in the Amazon, accounting for >20% of forest types vs <10% in the Amazon. The  
330 average curves changed shape with Amazon having more PAVD in the mid-canopy ~20m and  
331 Africa and SE Asia having more PAVD in the upper canopy ~30m. The less represented green  
332 and yellow structures increased by an absolute 3-4% over the Amazon and had much more  
333 PAVD (~0.05 increased PAVD) in the upper canopy (at ~30m height). River basins throughout  
334 the tropics had similar structural properties.

335 To explain the spatial patterns in the distributions of % one peak forests, we compared  
336 maps of percent one peak to a variety of datasets such as tree height (rh98), ecoregions, GEDI  
337 L4A AGBD, plant area index, number of footprints, climate (CWD, VPD, MMP,  $T_{\min}$ ), and total  
338 soils cation exchange capacity (Figure 7 – similar figure for Africa is Fig S5 and SE Asia Fig  
339 S6). The strongest correlations were with tree height and AGBD, with biomass a slightly better  
340 predictor for one peak forests (0.12 vs 0.14  $r^2$  respectively) (Figure 8). The AGBD L4A product  
341 is driven by tree height, so the similar strength of the correlations is not surprising, but there is a  
342 question of whether structure or tree height is a better predictor of biomass, which we discuss  
343 later. We compared meteorological data for VPD, PPT, CWD, PET,  $T_{\max}$  and  $T_{\min}$  to percent one  
344 peak and all were highly significant ( $P < 0.001$ ) but explained relatively little variance in the data.  
345  $T_{\max}$  explained the most at 5% of the variance, followed by VPD at 2.5% and the others  
346 explaining ~0.01 of the variance. Likewise, total cation exchange capacity was highly significant  
347 but again explained only about 1% of the variation (Figure 8). Other variables such as number of  
348 footprints was not related ( $r^2 < 0.01$ ), but PAI explained ~4% of variance, which is again, likely  
349 related to tree height. We then combined all climate and soil variables which explained ~9% of  
350 variance and the key parameters were  $T_{\max}$ , VPD followed by total cation exchange capacity.

351 Ecoregions, which may be a good proxy for floristics, delineated structure well for  
352 particular ecoregions. For instance, ecoregion 68 (Figure 7) had boundaries similar to  
353 boundaries of our structure dataset with a lower average value of percent one peak (75% vs 80%)  
354 than surrounding ecoregions. Another ecoregion with the boundary of the Pebas formation also  
355 delineated the structure data quite well. There were some regions that were partially delineated  
356 well but not entirely. For instance, even ecoregion 68 (Figure 7) had a sharp boundary in  
357 structure in the south not accounted for in the ecoregion.

358

## 359 Discussion

360 There are large changes in forest structure within the Amazon basin (60-90% one peak)  
361 and between the Amazon ( $79\pm 9$ sd) than SE Asia and Africa ( $72\pm 14$  v  $73\pm 11$  respectively). We  
362 are confident that the spatial patterns of structural changes are not mainly due to modern human  
363 influence, because we carefully screened for human influence using several independent remote  
364 sensed products (MODIS PFT (Friedl et al 2019), a Landsat based deforestation product  
365 (Hansen *et al.*, 2013) and GEDI tree height itself from GEDI (Dubayah *et al.*, 2020). Plot data  
366 from undisturbed regions (Doughty *et al.*, 2015) (DBH and tree height) showed similar structural  
367 trends in old growth plots (Figure 4). Human influence, as measured through forest integrity  
368 (Grantham *et al.*, 2020), also did not explain our geographic patterns of structure (Fig S2). The  
369 finding that the majority of GEDI footprints had a single PAI peak at  $\sim 15$ m was initially  
370 surprising. However, several tropical aircraft lidar campaigns showed similar shape for the  
371 lowland tropics (a single peak when averaged over  $\sim 1$  ha) but a slightly higher peak in PAI at  
372  $\sim 20$ m (Asner and Mascaro, 2014; Asner *et al.*, 2014). We hypothesize that the difference in the  
373 height of peak PAI may be due the difference in "energy return" profiles or how to correct for the  
374 reduced energy reaching the understory and the difficulty of laser pulses in the lower canopy  
375 returning due to an abundance of plant material. Full waveform information from GEDI can help  
376 correct for this energy return. In addition, prior work comparing TLS, LVIS and simulated  
377 GEDI data has found high-quality GEDI profiles on average to be accurate (Marselis *et al.*, 2018,  
378 2020). Finally, we are confident that the bulk of structural differences across the tropics are of  
379 natural origin because on top of the filters applied, some regions of the Amazon very far from  
380 human influence still had the dominance of one peak forests, such as the broad region north of  
381 Manaus in the Amazon (although there may be ancient legacy effects that we do not account for)  
382 (Fig S2).

383 The classic paradigm of "old growth" tropical forest architecture (visually represented in  
384 Fig 1 and figures in Halle et al 1980) is a generally closed upper canopy with large emergent  
385 trees at  $\sim 30$ - $35$ m where PAI peaks followed by a second peak at 15m with slightly lower PAI.  
386 These PAI peaks at  $\sim 15$  and 30m are occupied by "trees of the present" taking advantage of  
387 increased light cells (top of canopy and a second area of increased light at  $\sim 15$ m where  
388 lightflecks converge) (Halle, Oldeman and Tomlinson, 1980). This "classic paradigm" implies a  
389 stratified canopy that might be best represented by the green (2p\_uneq\_low) or yellow  
390 (2p\_uneq\_high) lines in Figs 2-5, but we find that this forest structure is relatively uncommon  
391 across the tropics making up just 3-6% of tropical forest area. In contrast, by far the most  
392 common PAVD profile across the tropics has a single peak in PAI density at 15m and this forest  
393 type likely reflects the absence of a closed upper canopy. In our color scheme (Figs 2-3), we can  
394 think of a gradually increasing proportion of vegetation percent in the upper canopy going from  
395 the highest PAI at the top with yellow (2p\_uneq\_high) (0.5% of total footprints), green  
396 (2p\_uneq\_low) (2%), red (2p\_eq\_high) (5%), magenta (2p\_eq\_low) (3%), and the lowest at blue  
397 (1 peak)(86%). Overall, these results show that a "stratified" forest with higher upper canopy  
398 closure is relatively rare across tropical forests.

399 Our structure maps broadly matched results from plot-based methods (Fig 4). We also  
400 found strong correlations between our structure maps and detailed maps of structure, floristics,  
401 climate and soils for a broad region of Central Africa from Fayolle et al 2014 where old growth  
402 *celtis* forest is associated with regions with more vertical layers (~60% 1 peak) while more  
403 degraded or young *celtis* forests with more pioneer species is associated with less structure (70%  
404 one peak) (Fayolle *et al.*, 2014). A floristic map for all of central Africa also showed correlations  
405 with our structure map (Réjou-Méchain *et al.*, 2021) with, for instance, north (more structure) to  
406 south (less structure) gradients in Central Africa (Figure 3) that match a transition in their figures  
407 from PCA 1, where floristics was controlled by a transition between cool, light-deficient forests  
408 and forests with high evapotranspiration rates, to PCA 2, where floristics were controlled more  
409 by seasonality and maximum temperature. In S.E. Asia, we compared our structure results to a  
410 logging gradient (Riutta *et al.*, 2018) with known structural changes and found GEDI footprints  
411 near Danum valley, where the tallest trees were found, also had some of the highest stratification  
412 (44% one peak) versus logged (78 % one peak) which gives further confidence in the results.  
413 Broadly, old growth forests in SE Asia have the highest levels of stratification and this may be  
414 partially due to the presence of Dipterocarps which are the tallest tropical trees (Shenkin *et al.*,  
415 2019; Jackson *et al.*, 2021).

416 Most of our independent datasets of soils or climate (as well as our combined model) did  
417 not strongly capture the spatial patterns of forest structure in the Amazon basin (Figure 7). Tree  
418 height and AGBD did match these patterns (Figure 8), but those variables cannot be considered  
419 independent of structure. However, patterns shown in Figure 4c in Figueiredo et al 2018 are  
420 similar to the one we highlight in this study (Fig 1) (Figueiredo *et al.*, 2018). Figueiredo et al  
421 (2018) created species distribution models for 40 species across the Amazon basin using 19  
422 bioclimatic variables, 19 soil variables, and four remote sensing variables (including GLAS  
423 derived canopy height (Simard *et al.*, 2011)). Overall, for most species, a combination of soils  
424 and climate variables explain most variance (similar to (Tuomisto *et al.*, 2019)) but single-  
425 variable models did poorly with an average of less than 8% of the variance explained. This  
426 broadly reflects our attempts to model structure with single variables. There was a tight  
427 correlation between regions with less structure (e.g. higher percentage of one peak) and areas  
428 where soils are the limiting factor to species occurrence, and regions with greater structure (i.e.  
429 lower percentage of 1peak) to areas where climate is the limiting factor to species occurrence.  
430 Perhaps deeper, more fertile soils allow for taller (either species or trees reaching their genetic  
431 height) and higher canopy closure forest types. Canopy height from the GLAS was the second  
432 most important variable for explaining species distributions, so it is possible that the Figueiredo  
433 et al (2018) map shows similar patterns to Fig 2 due to the inclusion of the height metric (a  
434 strong predictor of structure). A global study of forest structure based on upscaling terrestrial  
435 lidar with WorldClim2 datasets showed some correlations with our structure maps but also  
436 missed many of the regional changes (Ehbrecht *et al.*, 2021).

437 Ecoregions delineated boundaries in structural composition in a few key areas of the  
438 Amazon basin like the Pebas formation (Higgins *et al.*, 2011) and the Tapajos region in Para,  
439 Brazil (Figure 7). Higgins et al (2011) found a strong east-west gradient with an almost complete  
440 floristic turnover and an order of magnitude change in soil cation exchange capacity associated

441 with the presence of the Pebas formation (Higgins *et al.*, 2011). This line marking the boundary  
442 of the Pebas formation also seems to strongly delineate forest structure with one peak forest  
443 more abundant east of this line with lower cation exchange capacity and two peak forests more  
444 abundant to the west with higher cation exchange capacity. There is a further boundary  
445 delineated by the very wide (12-16 km) Tapajos River with forests to the west having a higher  
446 percentage one peak vs the eastern forests. Interestingly, some ecoregions (like 68) matched  
447 well with boundaries of vegetation structure, except for a few key areas (like in the south of  
448 region 68 – fig 7). This may indicate that forest structure could be used in the future to improve  
449 upon current ecoregion boundaries.

450         What causes the dominance of one peak forests in the tropics and the spatial changes in  
451 these patterns? A forest with a fully closed emergent canopy layer would have canopy layers, but  
452 most forests likely lack a fully closed upper layer, leading to the dominance of the one peak  
453 forests. Rephrasing the initial question, we can instead ask: Is the rarity of a closed upper layer  
454 canopy (or relative rareness of large emergent trees) due to the environment (soils or climate) or  
455 floristics (species composition)? In practice it is difficult to disentangle the floristic and  
456 environmental and there is a large literature describing how the environment (soils or climate)  
457 impacts the species composition. For instance, Amazonian species composition may follow a  
458 south-west/north-east soil fertility gradient and a north-west/south-east precipitation gradient (ter  
459 Steege *et al.*, 2006). Soil cation concentrations is the primary driver of floristic variation for  
460 trees (Tuomisto *et al.*, 2019) with climate being of secondary importance at regional scales.  
461 Environment alone could also directly impact tree height and structure, with hydraulic  
462 limitations or nutrient deficiencies causing trees to not being able to achieve their genetic height.  
463 Soil depth can impact structure as shallow soils can cause stunted root growth leading to a  
464 thinner upper canopy structure (Halle, Oldeman and Tomlinson, 1980).

465         What may explain the continental scale differences in structure between the Amazon and  
466 other tropical regions? Previous authors have noted large continental scale differences in AGBD  
467 and tree height (Borneo>Central Africa>Amazon) that broadly match the trends we show in  
468 structure (Feldpausch *et al.*, 2011; Lewis *et al.*, 2013). For instance, the Congo basin had  
469 average AGB values of 429 Mg ha<sup>-1</sup>, similar to Bornean forests (445 Mg ha<sup>-1</sup>), and much higher  
470 than the Amazon (289 Mg ha<sup>-1</sup>) (Lewis *et al.*, 2013). We show similar broad trends with the  
471 Amazon at 79±9sd % one peak and 25.6m height, SE Asia 72±14 and 28.7m height and Central  
472 Africa 73±11 and 28.5m. Lewis et al 2013 had hypothesized that AGBD differences between  
473 Amazon and Africa were due to different biomass residence times, the differences between  
474 Africa –Borneo differences were possibly due to NPP differences. However, tree height and  
475 biomass are structural attributes and do not explain the difference in continental structure.

476         To fully understand structural gradients across the Amazon, it is helpful to have higher  
477 resolution aircraft lidar. Asner et al 2014 flew aircraft lidar along an elevation and nutrient  
478 gradient in Peru and found that canopy height and shape (height of peak canopy volume divided  
479 by canopy height) had a high, negative correlation with gap density (Asner *et al.*, 2014).  
480 Perturbation, either up an elevation gradient or from high soil fertility to low, led to shorter  
481 forests with more gaps and a peak canopy volume at a lower height in the canopy. These changes

482 are broadly correlated with our maps of percentage of one peak, with perturbation (up elevation  
483 gradients or fertility gradients) increasing percentage of one peak forests. We found canopy  
484 stratification decreased as  $T_{\max}$  increased and soil fertility decreased (Fig 8). Therefore, our  
485 results support this paradigm that a movement away from ideal conditions may result in less  
486 structural complexity. Climate change will increase  $T_{\max}$ , but it is unclear whether this would  
487 further reduce structural complexity of tropical forests in the future.

488 In addition to tree height, remotely sensed leaf traits were also related to structure near  
489 some of our plots. Increased stratification (lower percentage of one peak) was significantly  
490 correlated ( $P < 0.05$ ) with increases in SLA, but this was almost entirely driven by low SLA  
491 values in high elevation plots and removing these plots removed the significant correlation  
492 (Malhi *et al.*, 2021). Along a logging gradient in Borneo (Riutta *et al.*, 2018), less stratification  
493 as logging increased was significantly correlated with an increase in SLA and foliar  
494 concentrations of phosphorus, similar to other studies (Baraloto *et al.*, 2012) (Carreño-Rocabado  
495 *et al.*, 2016). However, Both *et al.* 2019, a nearby field study, found a contrary result when  
496 comparing SLA along the forest gradient (Both *et al.*, 2019). Furthermore, Swinfield *et al.* 2019  
497 used high resolution aircraft hyperspectral data to predict SLA across the Bornean landscape  
498 (Swinfield *et al.*, 2019), but unlike most early studies (Doughty *et al.*, 2017) did not predict SLA  
499 accurately. Overall, we have reasons for caution for how well SLA can predict structure in  
500 tropical forests, but our abilities may improve in the future with hyperspectral satellites which  
501 could more accurately predict leaf traits at a global scale.

502 The primary goal of GEDI is to improve global predictions of biomass and incorporating  
503 structure could aid this goal. GEDI L4B was correlated ( $r^2 = 0.12$  and  $0.14$ ) with both tree height  
504 (rh 98) and structure (% one peak). The GEDI algorithm uses tree height (rh 98) as a metric to  
505 predict biomass, and since tree height is correlated with structure, the similar strength of the  
506 correlations is not surprising (Duncanson *et al.*, 2022). However, there is a question of whether  
507 structure in addition to tree height can be used to improve biomass predictions. The dominance  
508 of one peak forests likely indicates more open upper canopy forests and Asner and Mascaro  
509 (2014) have shown these forest types make biomass prediction more challenging (Asner and  
510 Mascaro, 2014). The plot data used to calibrate GEDI for tropical regions were not widely  
511 distributed throughout Amazonia, especially in the regions where height and structure diverge  
512 (Fig 2). Understanding why height and structure diverge in these regions may be key towards  
513 understanding whether structure can improve biomass predictions in the future.

514 Overall, over the majority of tropical forest area the upper canopy may be more open and  
515 tropical forest stratification is simpler than previously expected and this has important  
516 implications for predicting biomass. Furthermore, our results indicate that tropical forest  
517 canopies may be more open than previously thought which may expose animals to greater  
518 climate change related heat stress and require modifications to their behavior (Oliveira and  
519 Scheffers, 2019; Eppley *et al.*, 2022).

520

521 **Acknowledgements** - Support was provided by the GEDI mission and a NASA GEDI grant #  
522 20-GEDIST20-0020 and a NASA biodiversity grant # 80NSSC19K0206.

523 **Author contributions** – CED, AS, GK, HT, and CG designed the study. CED analyzed the RS  
524 data. JAG and YM contributed trait data. CED wrote the paper with contributions from all  
525 authors.

526

527 **Table 1** – Structure and trait data for regions surrounding plots from the GEM network (Malhi *et*  
528 *al.*, 2021). The columns are global region, RAINFOR plot code, plot structure classification for  
529 the footprint closest to the plot coordinates and the height of this footprint (highest vertical bin).  
530 Next is the average % one peak for footprints within 0.03° of the coordinates surrounding the  
531 plot and the average height of area. The last three columns are regionally averaged remotely  
532 sensed trait data (P=phosphorus=%, WD = wood density g cm<sup>-3</sup>, and SLA=specific leaf area - m<sup>2</sup>  
533 g<sup>-1</sup>)(Aguirre-Gutiérrez *et al.*, 2021).

Region	Rainfor code	Plot classification	height	% 1 peak near plot	Ave height	P	WD	SLA
SE Asia	DAN-04	magenta	80	0.21	60.75	0.1	0.61	0.01
SE Asia	DAN-05	blue	35	0.22	60	0.1	0.61	0.01
SE Asia	LAM-01	magenta	50	0.56	44.65	0.09	0.6	0.0105
SE Asia	LAM-02	magenta	50	0.44	50.55	0.1	0.59	0.0104
SE Asia	MLA-01	magenta	55	0.78	40	NaN	NaN	NaN
SE Asia	SAF-01	blue	45	0.88	42.65	0.1	0.58	0.0103
SE Asia	SAF-02	blue	40	0.71	44.2	0.1	0.59	0.0101
SE Asia	SAF-03	blue	40	0.8	44.2	0.1	0.58	0.0105
SE Asia	SAF-04	3-peak	95	0.53	61.9	0.1	0.6	0.0106
SE Asia	SAF-05	Blue	35	1	38.05	0.1	0.58	0.0102
W. Amazon	ALP11	yellow	45	0.82	40.8	0.1	0.61	0.01
W. Amazon	ALP30	blue	40	0.8	40.75	0.1	0.6	0.01
W. Amazon	SPD02	blue	45	0.78	46.95	0.1	0.6	0.009
W. Amazon	SPD01	blue	60	0.8	46.25	0.1	0.6	0.0091
W. Amazon	TRU08	blue	40	0.81	46.85	0.1	0.6	0.0089
W. Amazon	TRU07	blue	50	0.79	48.75	0.1	0.6	0.0089
W. Amazon	ESP01	blue	40	0.88	38.2	0.12	0.62	0.0075
W. Amazon	WAY01	blue	45	0.87	43.15	0.12	0.62	0.0074
W. Amazon	TRU03	blue	50	0.98	38.2	0.11	0.62	0.0076
W. Amazon	ACJ01	blue	30	0.89	39.25	0.12	0.62	0.0078
E. Amazon	CAX-03	blue	40	0.82	37.75	0.09	0.61	0.0102
E. Amazon	CAX-06	black	35	0	35	NaN	NaN	NaN
E. Amazon	STB-08	blue	45	0.69	44.55	0.09	0.61	0.0104
E. Amazon	STD-05	blue	40	0.81	35.2	0.08	0.65	0.0108
E. Amazon	STD-10	blue	40	0.94	38.45	0.09	0.62	0.0101
E. Amazon	STD-11	blue	30	0.85	38.7	0.08	0.61	0.0102
E. Amazon	STN-02	yellow	40	0.43	42.4	0.09	0.64	0.0104
E. Amazon	STN-04	blue	25	0.9	34.15	0.09	0.64	0.0103
E. Amazon	STN-06	blue	35	0.8	36.25	0.09	0.64	0.0102
E. Amazon	STN-09	blue	40	0.95	32.55	0.09	0.63	0.01
E. Amazon	STO-03	blue	45	0.7	44.1	0.08	0.66	0.0106
E. Amazon	STO-06	blue	35	0.89	43.55	0.08	0.65	0.0106
E. Amazon	STO-07	blue	40	0.73	43.75	0.08	0.66	0.0108

Gabon	IVI-01	blue	40	0.6	43.95	0.09	0.64	0.011
Gabon	IVI-02	blue	35	0.57	45.9	0.09	0.65	0.0109
Gabon	LPG-01	black	45	0.57	43.5	NaN	NaN	NaN
Gabon	LPG-02	blue	50	0.33	55.55	NaN	NaN	NaN
Gabon	MNG-04	blue	25	0.63	42	NaN	NaN	NaN

534

535

536

537

538 **Table 2** – Percent one peak forest of all GEDI footprints closest to the GEM plots and within a  
539 0.03° radius around the plot coordinates. Same as results from Table one, but averaged by  
540 continental region.

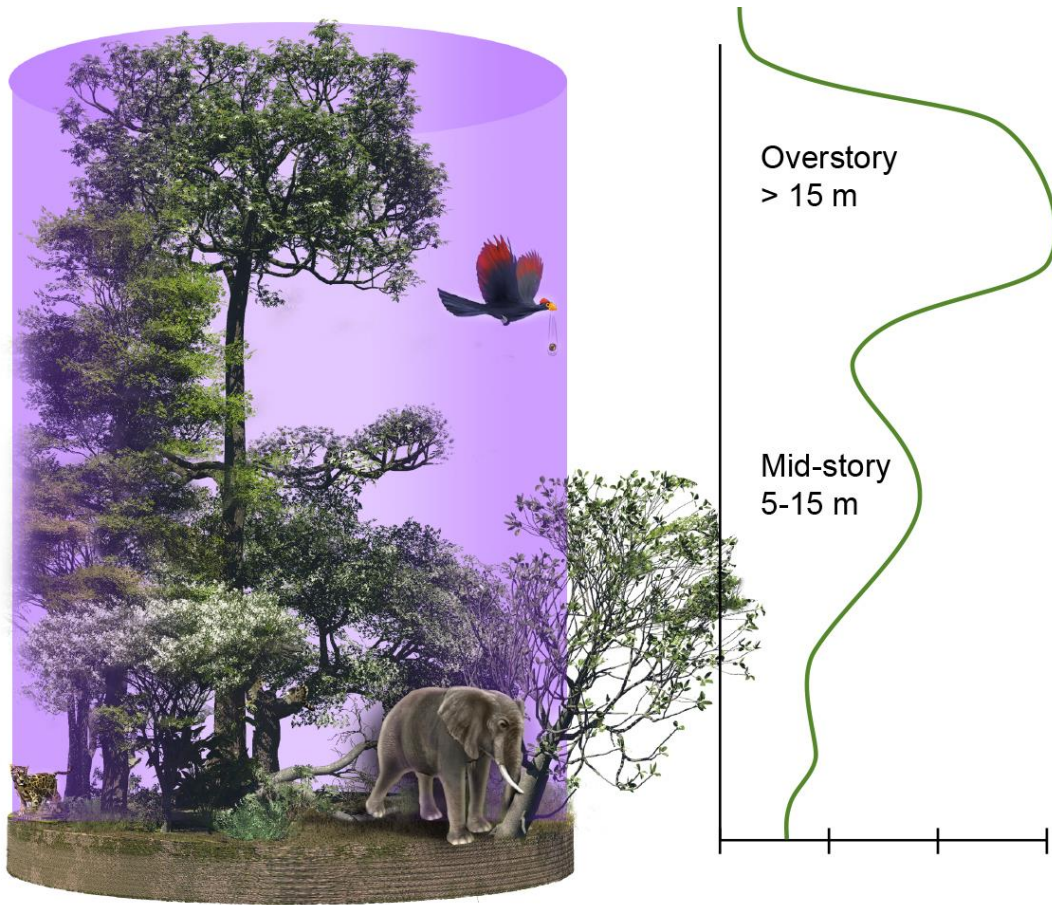
	<b>W. Amazon</b>	<b>E. Amazon</b>	<b>Gabon</b>	<b>SE Asia</b>
<b>Nearest to plot</b>	90%	85%	80%	50%
<b>Close to plot</b>	84%	79%	54%	61%

541

542

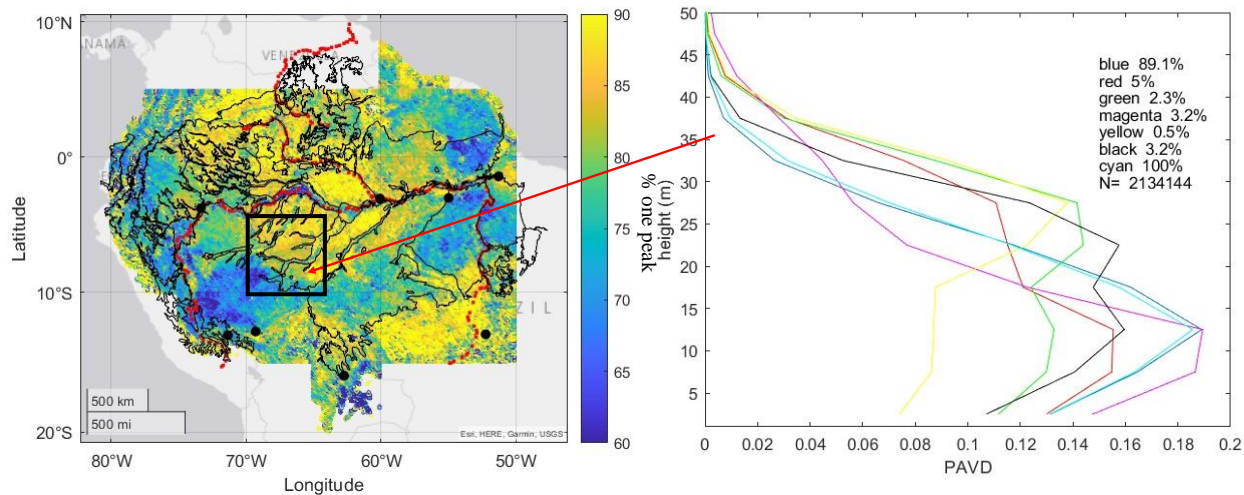
543

544 **Figures**



545

546 **Figure 1** – Artistic rendition of a “typical” stratified tropical forest with the forest on left within  
547 a 25m diameter GEDI pulse and the expected layered return of the profile on the right. Animals  
548 in figure show how animals both impact and are impacted by canopy structure.

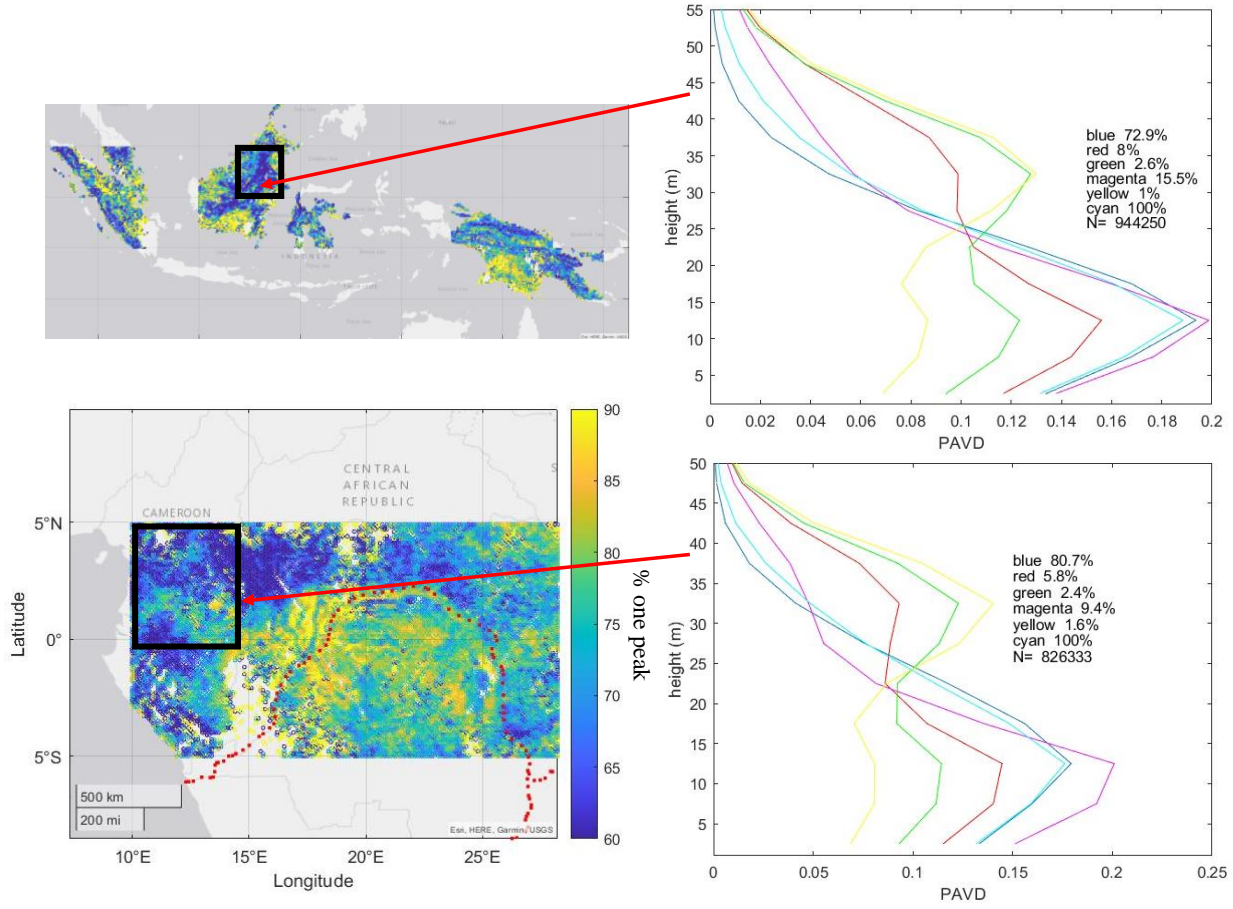


549

550 **Figure 2** – (left) Each pixel represents the number of one peak footprints divided by total  
 551 number of GEDI footprints in a 0.1 by 0.1 degree region for Amazonia. Black lines are  
 552 ecoregions for the Amazon region. Red lines are rivers and black dots are field plots used in  
 553 Figure 4. (right) Average waveforms for the region in the black box. We give the total number of  
 554 individual footprints analyzed and the percentage for each type. PAVD is plant area volume  
 555 density. Cyan is the average waveform for all data (100%) in the black box.

556

557



559

560 **Figure 3** – (left) Each pixel represents the number of one peak footprints divided by total GEDI  
 561 footprints in a 0.1 by 0.1 degree region for SE Asia (top) and Central Africa (bottom). Red lines  
 562 are major rivers. (right) Average vertical footprints for the region in the black box. For each type  
 563 we give the percentage and the total number of individual footprints analyzed. Averages  
 564 representing <1% were removed. PAVD is plant area volume density. Cyan is the average  
 565 waveform for all data (100%) in the black box.

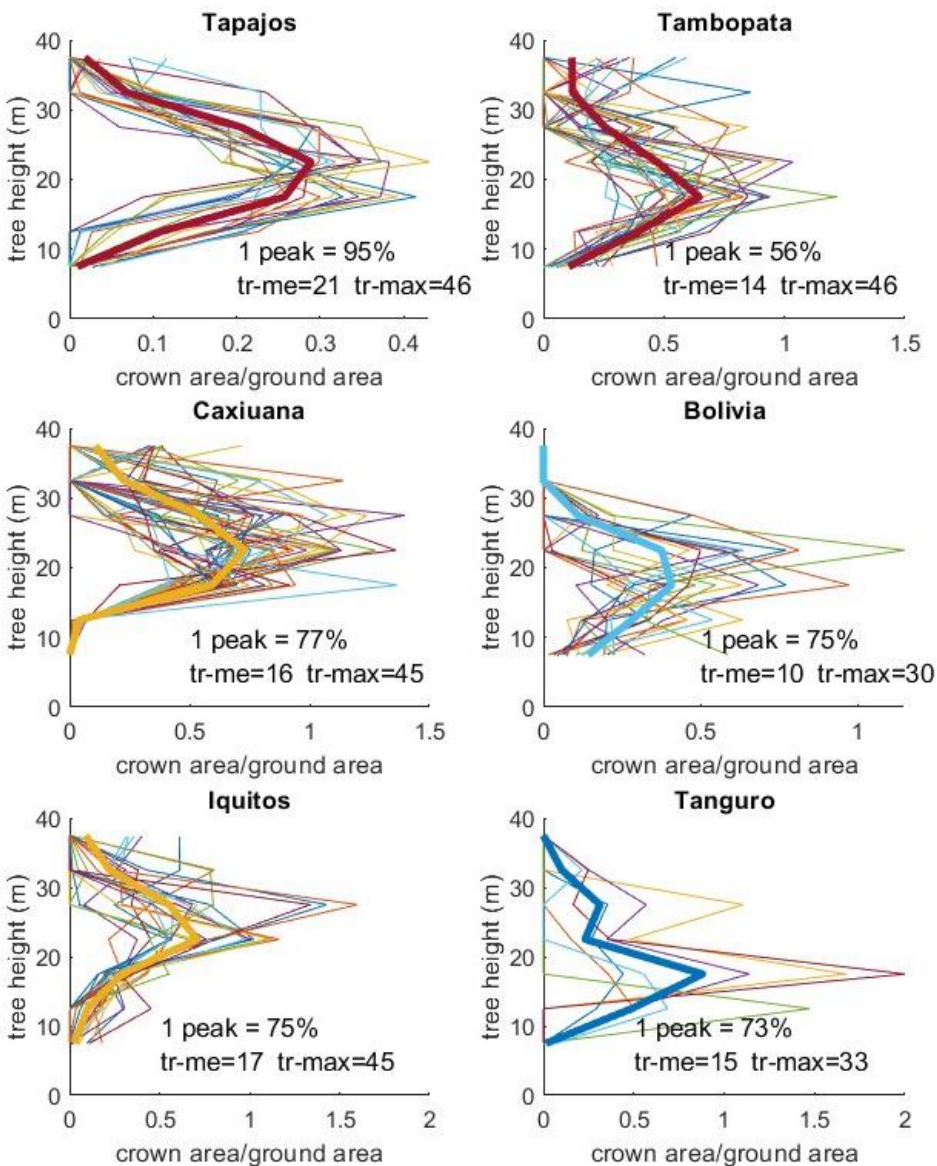
566

567

568

569

570

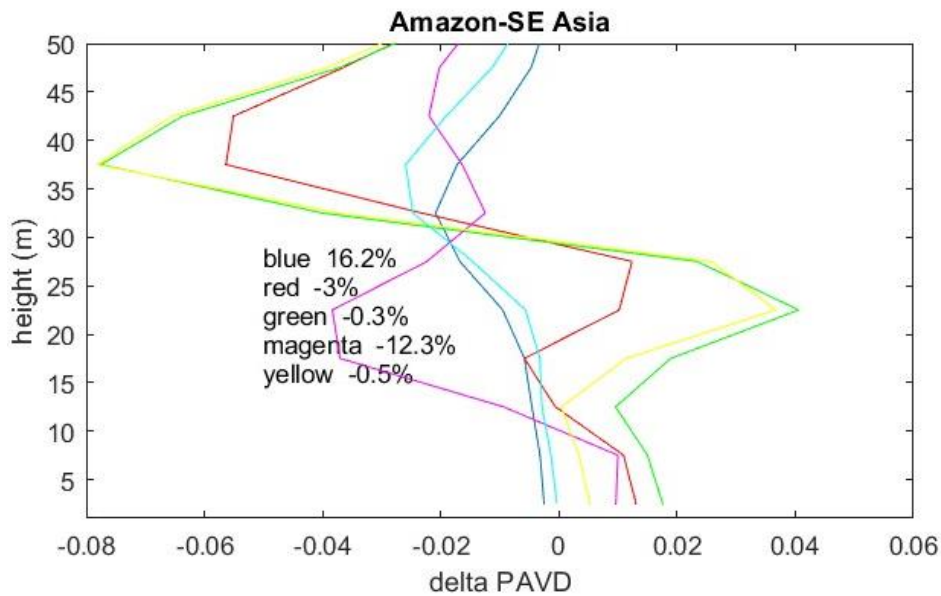
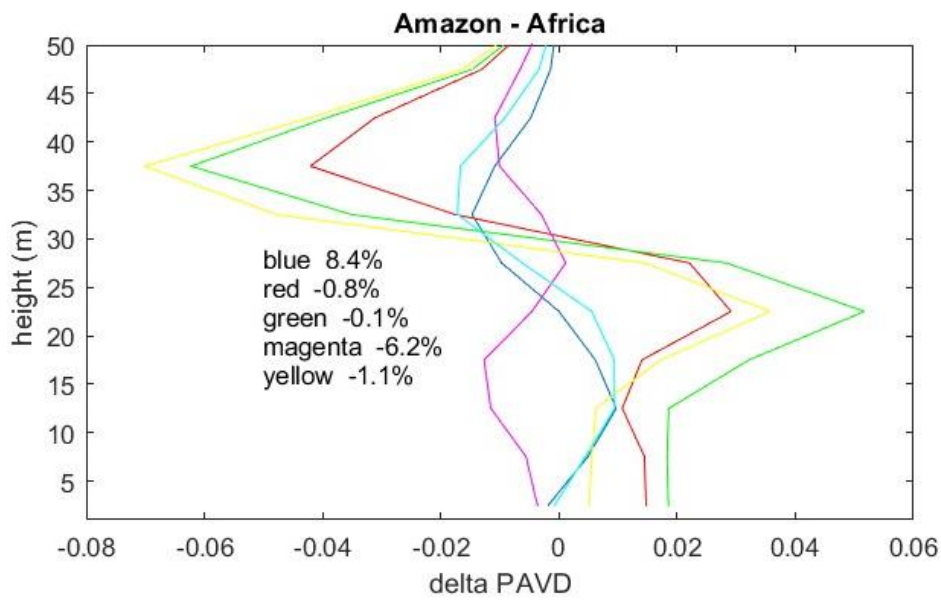


571

572 **Figure 4** – Tree height versus crown area/ground area as estimated with plot level tree DBH and  
573 tree height for six regions as shown in Figure one (Tapajos – 18ha, Caxiuana 4 ha, Tambopata 2  
574 ha, Iquitos 2 ha, Bolivia 2 ha, Tanguro 1 ha). Thin lines are groups of 50 trees and the bold line  
575 is the plot average. For each 5-meter tree height bin we estimate crown diameter following  
576 Asner et al 2002. We then use the same “peak” procedure as with GEDI data to estimate one vs  
577 two peak forests and show this as a percentage. We also show median (tr-me) and maximum  
578 tree height (tr-max) for the plots. Results from the Tapajos are for trees >25cm DBH only.

579

580



581

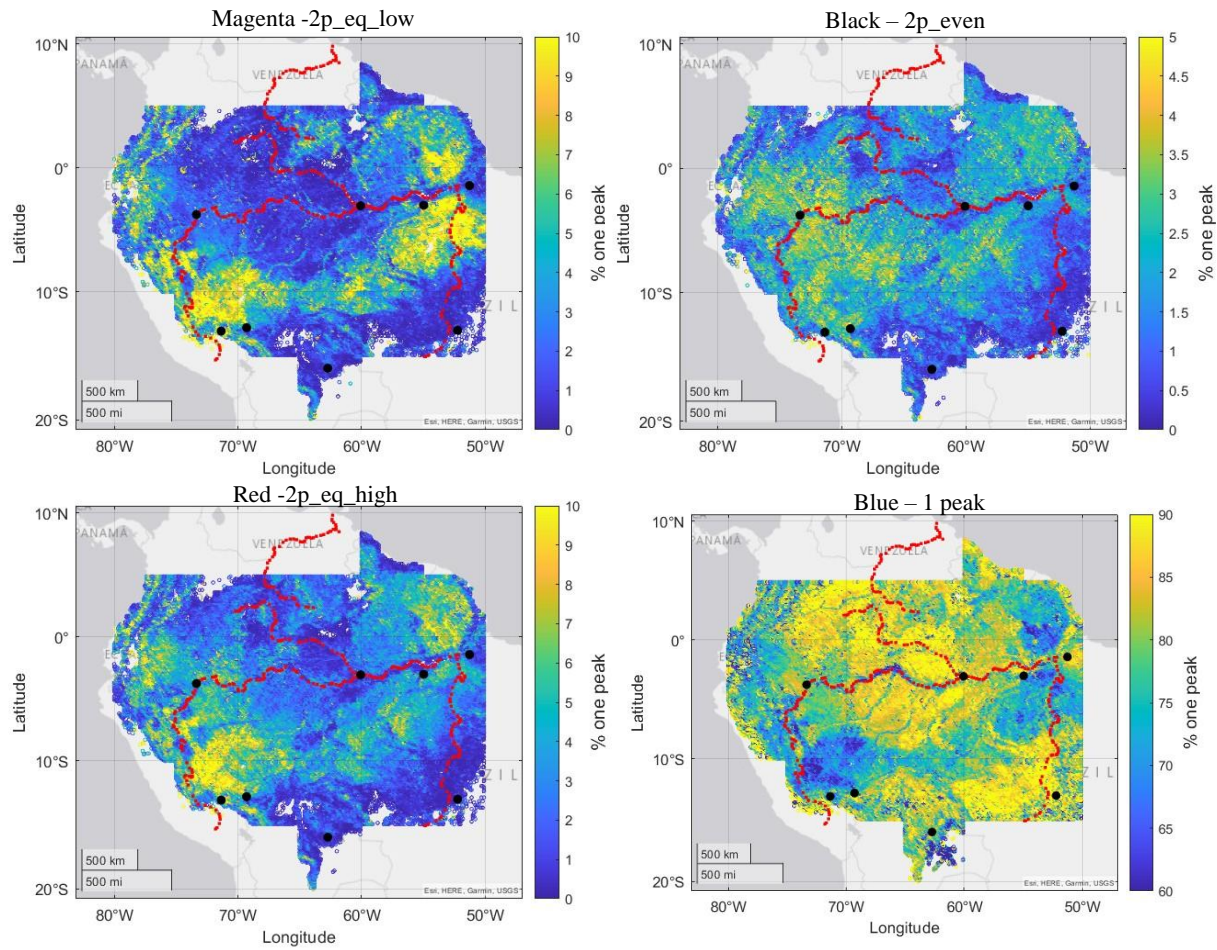
582 **Figure 5** – The change in the average forest structure between the Amazon and Africa (top) and  
583 the Amazon and SE Asia (bottom) for the regions highlighted in black in Fig 2-3. The numbers  
584 are the listed differences in the percentage abundance.

585

586

587

588



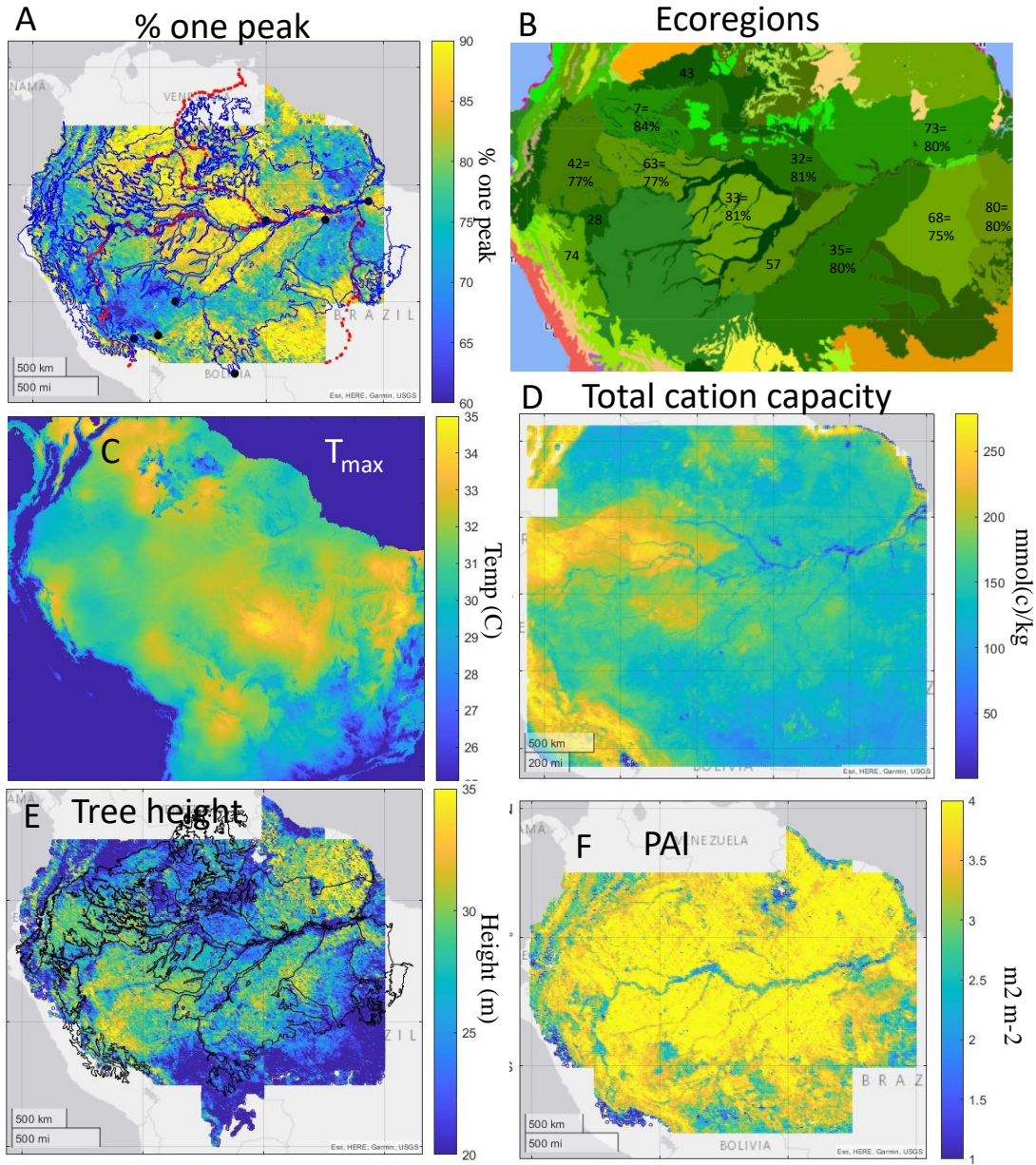
589

590 **Figure 6** – Spatial distributions for the Amazon basin for different types of the “2 peak” forests.  
591 The color labels are associated with the colors of the lines in Figs 2-3. The colorbar scales are  
592 different between panels.

593

594

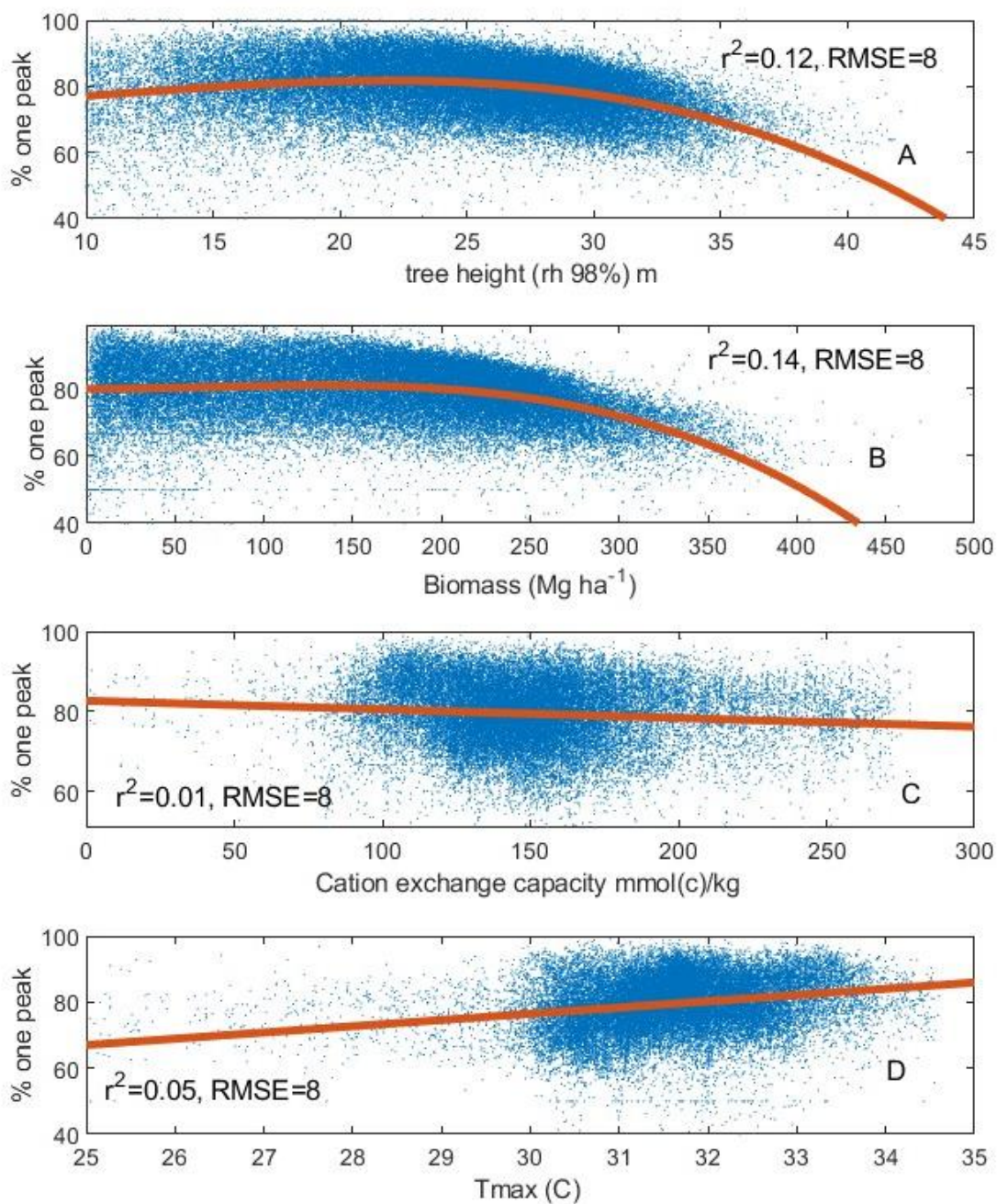
595  
596  
597



598

599 **Figure 7** – Different data layers that were used for comparison with the percent one peak dataset.  
600 (A) Spatial distribution of the percentage of one peak forests (same as figure 1) with the  
601 ecoregions of the Amazon basin overlaid (Olsen et al 2001). (B) A map of the ecoregions alone  
602 shown above for clarity with percent one peak for each ecoregion. (C) Max temperature -  $T_{max}$   
603 ( $^{\circ}C$ ), (D) total cation exchange capacity (mmol(c)/kg), (E) median tree height from rh98 GEDI  
604 with ecoregions, and (F) plant area index from GEDI.

605



606

607 **Figure 8** –(A) Tree height (rh98%), (B) AGBD from GEDI L4B, (C) cation exchange capacity  
608 ( $\text{mmol(c)/kg}$  and (D)  $T_{\text{max}}$  ( $^{\circ}\text{C}$ ) vs percent one peak forests for the Amazon basin. For each we  
609 show  $r^2$  and RMSE.

610

611

612 **References**

- 613 Abatzoglou, J. T. *et al.* (2018) ‘TerraClimate, a high-resolution global dataset of monthly climate  
614 and climatic water balance from 1958–2015’, *Scientific Data*, 5(1), p. 170191. doi:  
615 10.1038/sdata.2017.191.
- 616 Aguirre-Gutiérrez, J. *et al.* (2021) ‘Pantropical modelling of canopy functional traits using  
617 Sentinel-2 remote sensing data’, *Remote Sensing of Environment*, 252, p. 112122. doi:  
618 <https://doi.org/10.1016/j.rse.2020.112122>.
- 619 Asner, G. P. *et al.* (2014) ‘Landscape-scale changes in forest structure and functional traits along  
620 an Andes-to-Amazon elevation gradient’, *Biogeosciences*, 11(3), pp. 843–856. doi: 10.5194/bg-  
621 11-843-2014.
- 622 Asner, G. P. and Mascaro, J. (2014) ‘Mapping tropical forest carbon: Calibrating plot estimates  
623 to a simple LiDAR metric’, *Remote Sensing of Environment*, 140, pp. 614–624. doi:  
624 <https://doi.org/10.1016/j.rse.2013.09.023>.
- 625 Baker, P. J. and Wilson, J. S. (2000) ‘A quantitative technique for the identification of canopy  
626 stratification in tropical and temperate forests’, *Forest Ecology and Management*, 127(1), pp.  
627 77–86. doi: [https://doi.org/10.1016/S0378-1127\(99\)00118-8](https://doi.org/10.1016/S0378-1127(99)00118-8).
- 628 Baraloto, C. *et al.* (2012) ‘Contrasting taxonomic and functional responses of a tropical tree  
629 community to selective logging’, *Journal of Applied Ecology*. John Wiley & Sons, Ltd, 49(4),  
630 pp. 861–870. doi: <https://doi.org/10.1111/j.1365-2664.2012.02164.x>.
- 631 Batjes, N. H., Ribeiro, E. and van Oostrum, A. (2020) ‘Standardised soil profile data to support  
632 global mapping and modelling (WoSIS snapshot 2019)’, *Earth System Science Data*, 12(1), pp.  
633 299–320. doi: 10.5194/essd-12-299-2020.
- 634 Both, S. *et al.* (2019) ‘Logging and soil nutrients independently explain plant trait expression in  
635 tropical forests’, *New Phytologist*. doi: 10.1111/nph.15444.
- 636 Burns, P. *et al.* (2020) ‘Incorporating canopy structure from simulated GEDI lidar into bird  
637 species distribution models’, *Environmental Research Letters*. IOP Publishing, 15(9), p. 95002.  
638 doi: 10.1088/1748-9326/ab80ee.
- 639 Carreño-Rocabado, G. *et al.* (2016) ‘Land-use intensification effects on functional properties in  
640 tropical plant communities’, *Ecological Applications*. John Wiley & Sons, Ltd, 26(1), pp. 174–  
641 189. doi: <https://doi.org/10.1890/14-0340>.
- 642 Doughty, C. E. *et al.* (2015) ‘Drought impact on forest carbon dynamics and fluxes in  
643 Amazonia’, *Nature*. doi: 10.1038/nature14213.
- 644 Doughty, C. E. *et al.* (2017) ‘Can Leaf Spectroscopy Predict Leaf and Forest Traits Along a  
645 Peruvian Tropical Forest Elevation Gradient?’, *Journal of Geophysical Research:*  
646 *Biogeosciences*. doi: 10.1002/2017JG003883.
- 647 Dubayah, R. *et al.* (2020) ‘The Global Ecosystem Dynamics Investigation: High-resolution laser  
648 ranging of the Earth’s forests and topography’, *Science of Remote Sensing*. doi:

649 10.1016/j.srs.2020.100002.

650 Duncanson, L. *et al.* (2022) ‘Aboveground biomass density models for NASA’s Global  
651 Ecosystem Dynamics Investigation (GEDI) lidar mission’, *Remote Sensing of Environment*, 270,  
652 p. 112845. doi: <https://doi.org/10.1016/j.rse.2021.112845>.

653 Ehbrecht, M. *et al.* (2021) ‘Global patterns and climatic controls of forest structural complexity’,  
654 *Nature Communications*, 12(1), p. 519. doi: 10.1038/s41467-020-20767-z.

655 Eppley, T. M. *et al.* (2022) ‘Factors influencing terrestriality in primates of the Americas and  
656 Madagascar’, *Proceedings of the National Academy of Sciences*. Proceedings of the National  
657 Academy of Sciences, 119(42), p. e2121105119. doi: 10.1073/pnas.2121105119.

658 Fayolle, A. *et al.* (2014) ‘A new insight in the structure, composition and functioning of central  
659 African moist forests’, *Forest Ecology and Management*, 329, pp. 195–205. doi:  
660 <https://doi.org/10.1016/j.foreco.2014.06.014>.

661 Feldpausch, T. R. *et al.* (2011) ‘Height-diameter allometry of tropical forest trees’,  
662 *Biogeosciences*, 8(5), pp. 1081–1106. doi: 10.5194/bg-8-1081-2011.

663 Figueiredo, F. O. G. *et al.* (2018) ‘Beyond climate control on species range: The importance of  
664 soil data to predict distribution of Amazonian plant species’, *Journal of Biogeography*. John  
665 Wiley & Sons, Ltd, 45(1), pp. 190–200. doi: <https://doi.org/10.1111/jbi.13104>.

666 Grantham, H. S. *et al.* (2020) ‘Anthropogenic modification of forests means only 40% of  
667 remaining forests have high ecosystem integrity’, *Nature Communications*, 11(1), p. 5978. doi:  
668 10.1038/s41467-020-19493-3.

669 Halle, F., Oldeman, R. and Tomlinson, P. (1980) *Tropical Trees and Forests: An Architectural  
670 Analysis*. New York: Springer.

671 Hansen, M. C. *et al.* (2013) ‘High-Resolution Global Maps of 21st-Century Forest Cover  
672 Change’, *Science*. American Association for the Advancement of Science, 342(6160), pp. 850–  
673 853. doi: 10.1126/science.1244693.

674 Higgins, M. A. *et al.* (2011) ‘Geological control of floristic composition in Amazonian forests’,  
675 *Journal of Biogeography*. John Wiley & Sons, Ltd, 38(11), pp. 2136–2149. doi:  
676 <https://doi.org/10.1111/j.1365-2699.2011.02585.x>.

677 Jackson, T. D. *et al.* (2021) ‘The mechanical stability of the world’s tallest broadleaf trees’,  
678 *Biotropica*. John Wiley & Sons, Ltd, 53(1), pp. 110–120. doi: <https://doi.org/10.1111/btp.12850>.

679 Kays, R. and Allison, A. (2001) ‘Arboreal tropical forest vertebrates: current knowledge and  
680 research trends BT - Tropical Forest Canopies: Ecology and Management: Proceedings of ESF  
681 Conference, Oxford University, 12–16 December 1998’, in Linsenmair, K. E. *et al.* (eds).  
682 Dordrecht: Springer Netherlands, pp. 109–120. doi: 10.1007/978-94-017-3606-0\_9.

683 Krieger, G. *et al.* (2007) ‘TanDEM-X: A Satellite Formation for High-Resolution SAR  
684 Interferometry’, *IEEE Transactions on Geoscience and Remote Sensing*, 45(11), pp. 3317–3341.  
685 doi: 10.1109/TGRS.2007.900693.

686 Lewis, S. L. *et al.* (2013) ‘Above-ground biomass and structure of 260 African tropical forests’,

687 *Philosophical Transactions of the Royal Society B: Biological Sciences*. doi:  
688 10.1098/rstb.2012.0295.

689 Maclean, I. M. D. and Klinges, D. H. (2021) ‘Microclimc: A mechanistic model of above, below  
690 and within-canopy microclimate’, *Ecological Modelling*, 451, p. 109567. doi:  
691 <https://doi.org/10.1016/j.ecolmodel.2021.109567>.

692 Malhi, Y. *et al.* (2021) ‘The Global Ecosystems Monitoring network: Monitoring ecosystem  
693 productivity and carbon cycling across the tropics’, *Biological Conservation*, 253, p. 108889.  
694 doi: <https://doi.org/10.1016/j.biocon.2020.108889>.

695 Marselis, S. M. *et al.* (2018) ‘Distinguishing vegetation types with airborne waveform lidar data  
696 in a tropical forest-savanna mosaic: A case study in Lopé National Park, Gabon’, *Remote  
697 Sensing of Environment*, 216, pp. 626–634. doi: <https://doi.org/10.1016/j.rse.2018.07.023>.

698 Marselis, S. M. *et al.* (2020) ‘Evaluating the potential of full-waveform lidar for mapping pan-  
699 tropical tree species richness’, *Global Ecology and Biogeography*. John Wiley & Sons, Ltd,  
700 29(10), pp. 1799–1816. doi: <https://doi.org/10.1111/geb.13158>.

701 Oliveira, B. F. and Scheffers, B. R. (2019) ‘Vertical stratification influences global patterns of  
702 biodiversity’, *Ecography*. John Wiley & Sons, Ltd, 42(2), p. 249. doi:  
703 <https://doi.org/10.1111/ecog.03636>.

704 Olson, D. M. *et al.* (2001) ‘Terrestrial Ecoregions of the World: A New Map of Life on Earth: A  
705 new global map of terrestrial ecoregions provides an innovative tool for conserving biodiversity’,  
706 *BioScience*, 51(11), pp. 933–938. doi: 10.1641/0006-3568(2001)051[0933:TEOTWA]2.0.CO;2.

707 Palminteri, S. and Peres, C. A. (2012) ‘Habitat Selection and Use of Space by Bald-Faced Sakis  
708 (*Pithecia irrorata*) in Southwestern Amazonia: Lessons from a Multiyear, Multigroup Study’,  
709 *International Journal of Primatology*, 33(2), pp. 401–417. doi: 10.1007/s10764-011-9573-0.

710 Réjou-Méchain, M. *et al.* (2021) ‘Unveiling African rainforest composition and vulnerability to  
711 global change’, *Nature*, 593(7857), pp. 90–94. doi: 10.1038/s41586-021-03483-6.

712 Richards, P. W. (1952) *The Tropical Rain Forest*. Cambridge University Press.

713 Riutta, T. *et al.* (2018) ‘Logging disturbance shifts net primary productivity and its allocation in  
714 Bornean tropical forests’, *Global Change Biology*. John Wiley & Sons, Ltd (10.1111), 24(7), pp.  
715 2913–2928. doi: 10.1111/gcb.14068.

716 Shenkin, A. *et al.* (2019) ‘The World’s Tallest Tropical Tree in Three Dimensions’, *Frontiers in  
717 Forests and Global Change*, 2. doi: 10.3389/ffgc.2019.00032.

718 Simard, M. *et al.* (2011) ‘Mapping forest canopy height globally with spaceborne lidar’, *Journal  
719 of Geophysical Research: Biogeosciences*. doi: 10.1029/2011JG001708.

720 Smith, A. P. (1973) ‘Stratification of Temperature and Tropical Forests’, *The American  
721 Naturalist*. The University of Chicago Press, 107(957), pp. 671–683. doi: 10.1086/282866.

722 ter Steege, H. *et al.* (2006) ‘Continental-scale patterns of canopy tree composition and function  
723 across Amazonia’, *Nature*, 443(7110), pp. 444–447. doi: 10.1038/nature05134.

724 Stork, N. E. (2018) ‘How Many Species of Insects and Other Terrestrial Arthropods Are There

725 on Earth?', *Annual Review of Entomology*. Annual Reviews, 63(1), pp. 31–45. doi:  
726 10.1146/annurev-ento-020117-043348.

727 Swinfield, T. *et al.* (2019) 'Imaging spectroscopy reveals the effects of topography and logging  
728 on the leaf chemistry of tropical forest canopy trees', *Global Change Biology*. John Wiley &  
729 Sons, Ltd (10.1111), n/a(n/a). doi: 10.1111/gcb.14903.

730 Tang, H. *et al.* (2016) 'Characterizing leaf area index (LAI) and vertical foliage profile (VFP)  
731 over the United States', *Biogeosciences*, 13(1), pp. 239–252. doi: 10.5194/bg-13-239-2016.

732 Tang, H. and Dubayah, R. (2017) 'Light-driven growth in Amazon evergreen forests explained  
733 by seasonal variations of vertical canopy structure', *Proceedings of the National Academy of  
734 Sciences*. Proceedings of the National Academy of Sciences, 114(10), pp. 2640–2644. doi:  
735 10.1073/pnas.1616943114.

736 Taubert, F. *et al.* (2021) 'Deriving Tree Size Distributions of Tropical Forests from Lidar',  
737 *Remote Sensing*. doi: 10.3390/rs13010131.

738 Terborgh, J. (1992) 'Maintenance of Diversity in Tropical Forests', *Biotropica*. [Association for  
739 Tropical Biology and Conservation, Wiley], 24(2), pp. 283–292. doi: 10.2307/2388523.

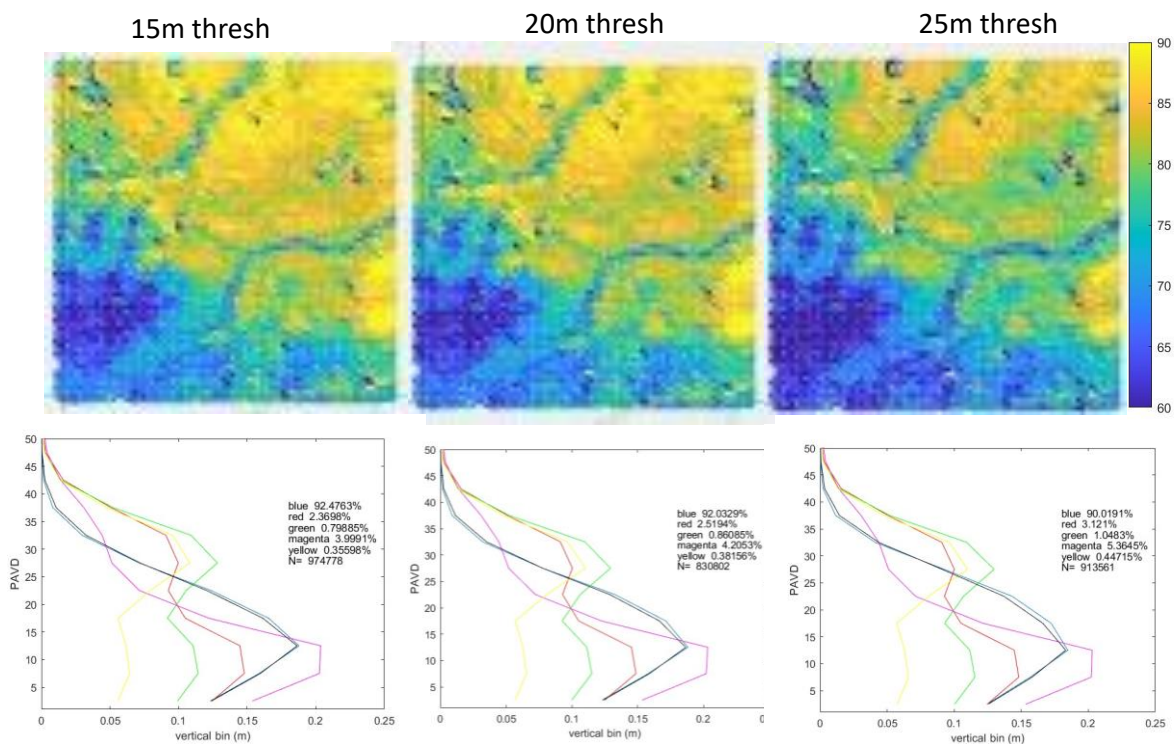
740 Tuomisto, H. *et al.* (2019) 'Discovering floristic and geocological gradients across Amazonia',  
741 *Journal of Biogeography*. John Wiley & Sons, Ltd, 46(8), pp. 1734–1748. doi:  
742 <https://doi.org/10.1111/jbi.13627>.

743

744

745

## Supplementary Figures

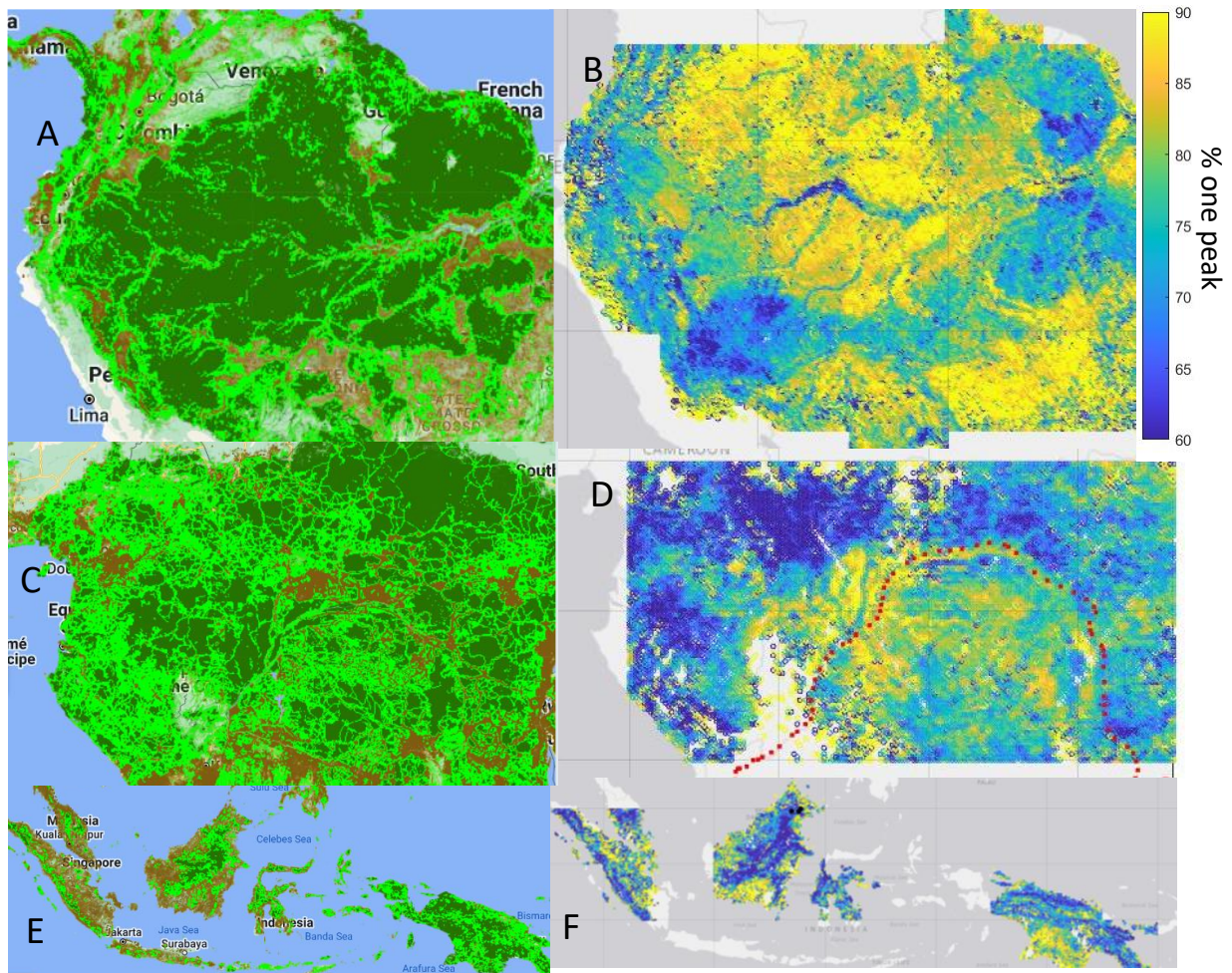


746

747 **Figure S1** – (top) A map of % one peak forests in a 5 by 5 degree region of the Amazon where  
748 we modified our relative height metric 98% with a lower threshold of 15, 20, and 25m. (bottom)  
749 The different PAVD profiles for each threshold similar to fig 2.

750

751

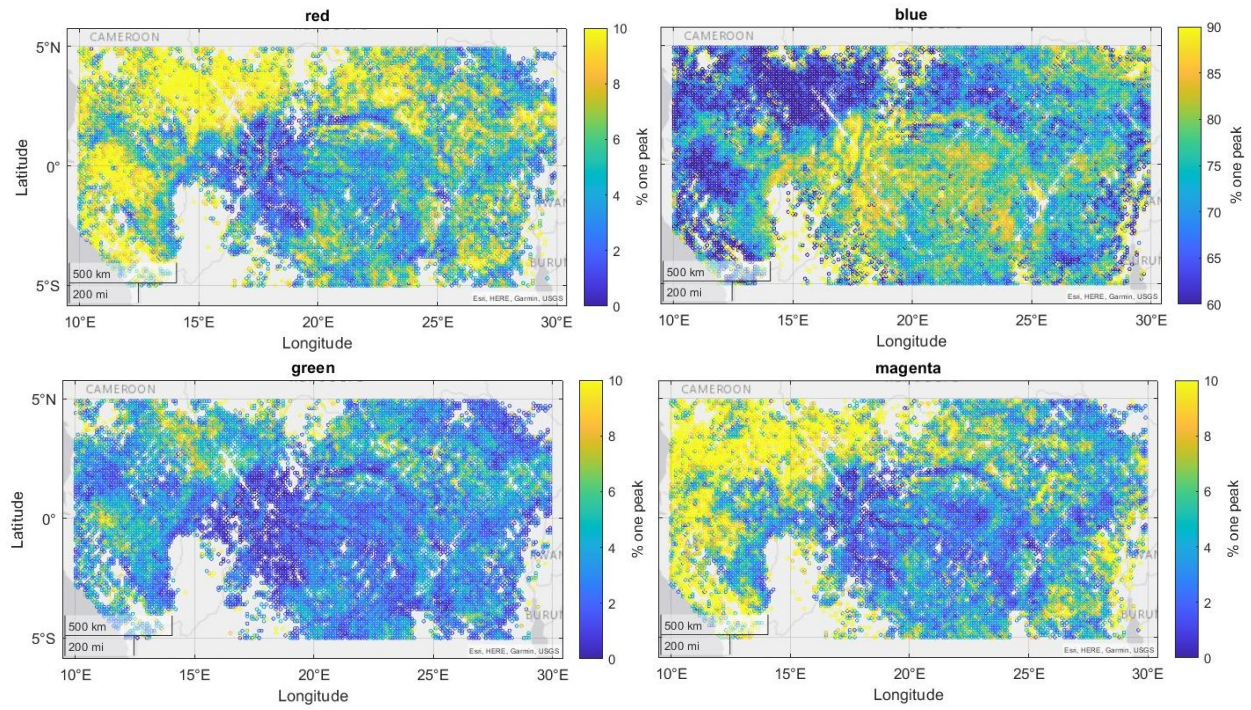


752

753 **Figure S2** – A comparison of one peak forest types for (B) Amazonia, (D) Central Africa, and  
 754 (F) SE Asia to an index of forest integrity as determined by degree of anthropogenic  
 755 modification from <https://www.forestintegrity.com/> (Grantham *et al.*, 2020) for (A) Amazonia,  
 756 (C) Central Africa, and (E) SE Asia where the darkest greens are areas with the least human  
 757 disturbance.

758

759



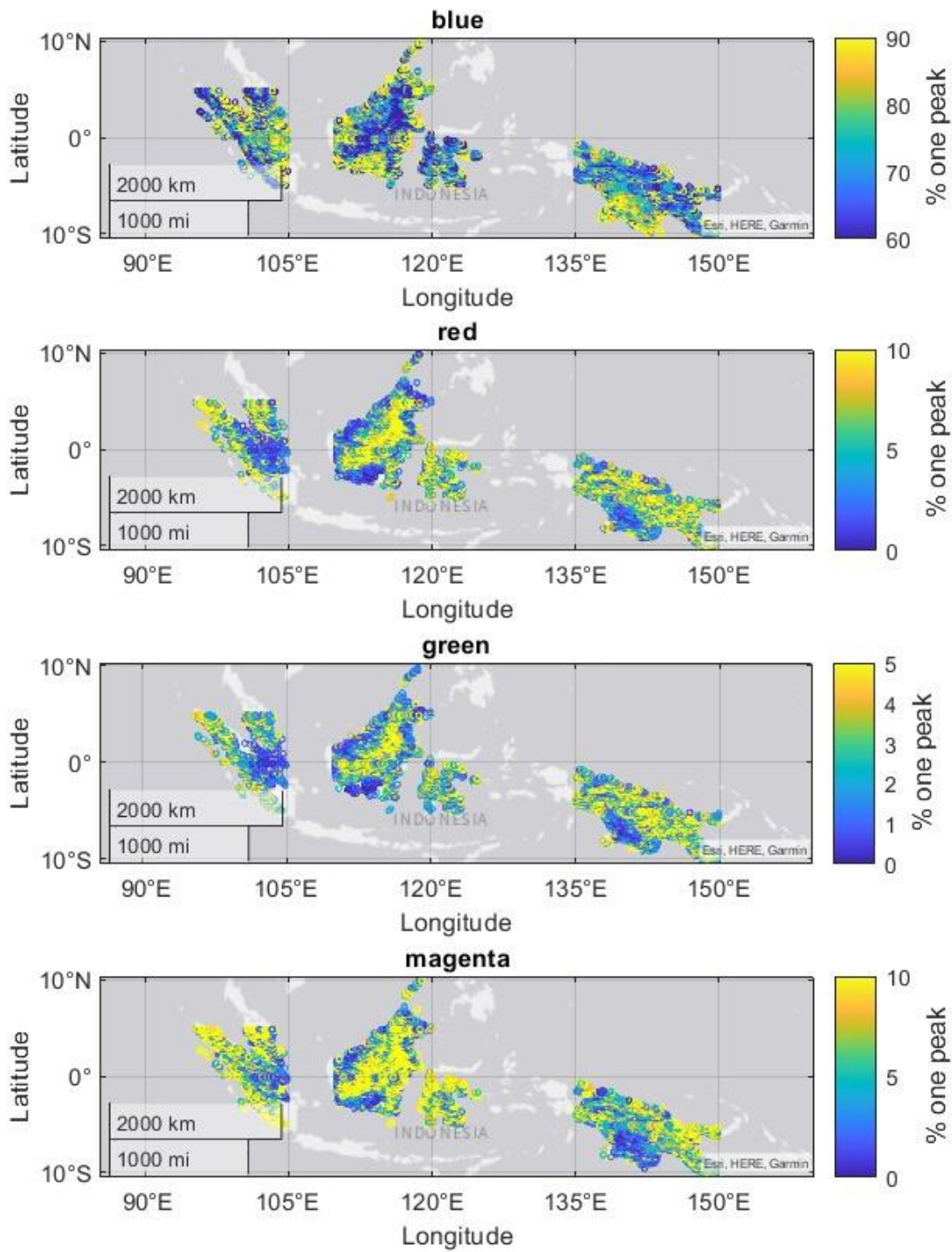
760

761 **Figure S3 -** Spatial distributions for different types of Central African “two peak” forests. The  
 762 color labels are associated with the colors of the lines in Figs 2-3.

763

764

765



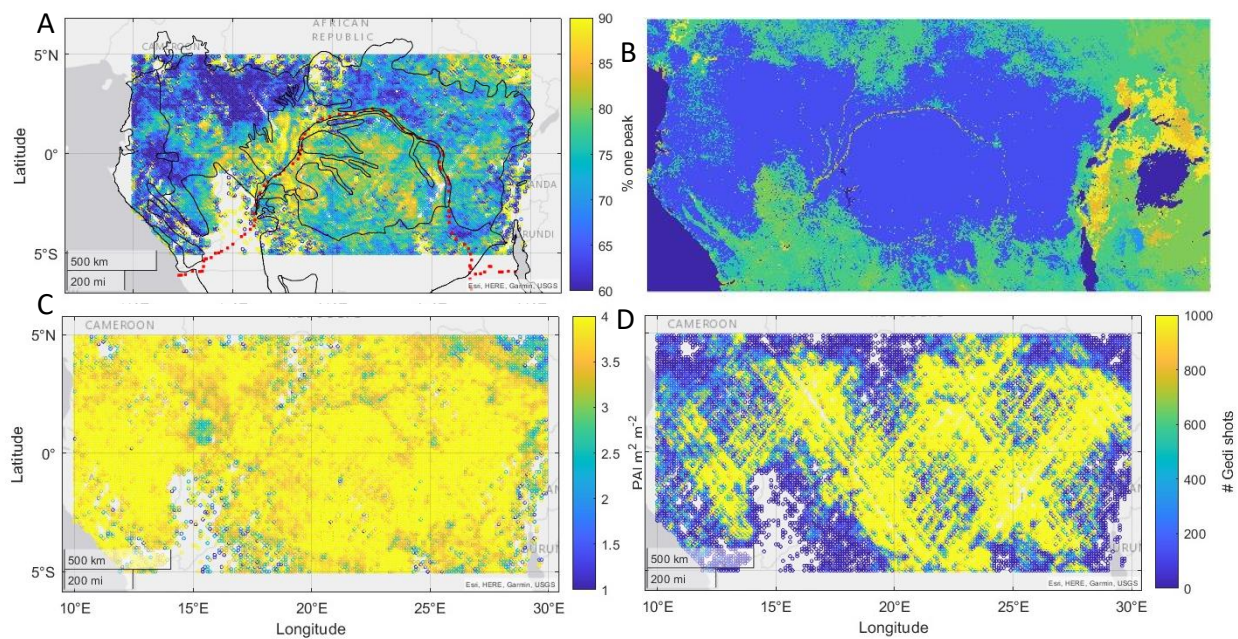
766

767 **Figure S4** - Spatial distributions for different types of SE Asian “two peak” forests. The color  
 768 labels are associated with the colors of the lines in Figs 2-3.

769

770

771

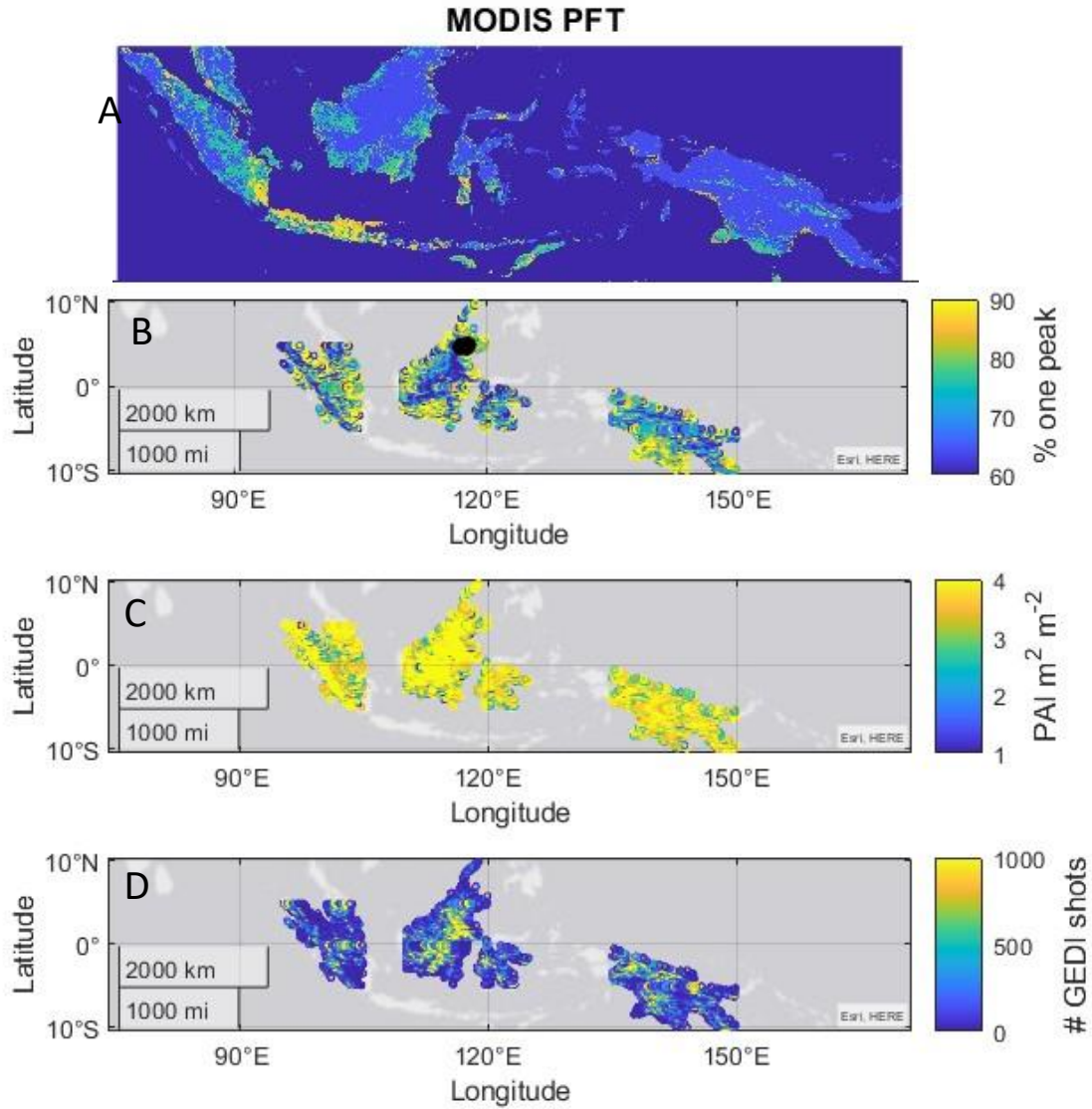


772

773 **Figure S5** - Different data layers for Central Africa. (A) Spatial distribution of the percentage of  
774 1 peak forests (same as figure 3) with ecoregions overlaid. (B) MODIS PFT classification with  
775 the light blue representing broadleaf tropical evergreen PFT. (C) Plant area index from GEDI  
776 and (D) # of GEDI shots per 0.1 by 0.1 pixel.

777

778



779

780 **Figure S6** - Different data layers for SE Asia. (A) MODIS PFT classification with the light blue  
 781 representing broadleaf tropical evergreen PFT. (B) Spatial distribution of the percentage of 1  
 782 peak forests (same as figure 3). (C) Plant area index from GEDI and (D) # of GEDI shots  
 783 by 0.1 by 0.1 pixel.

784

785

786